


## Article

# The Prostate Cancer Therapy Enzalutamide Compared with Abiraterone Acetate/Prednisone Impacts Motivation for Exploration, Spatial Learning and Alters Dopaminergic Transmission in Aged Castrated Mice

Celeste Nicola <sup>1,2,3,†</sup>, Martine Dubois <sup>1,2,3,†</sup>, Cynthia Campart <sup>1,2,3</sup>, Tareq Al Sagheer <sup>1,2</sup>, Laurence Desrues <sup>1,2,3</sup>, Damien Schapman <sup>2,4</sup>, Ludovic Galas <sup>2,4</sup>, Marie Lange <sup>3,5,6</sup>, Florence Joly <sup>3,5,6,7</sup> and H el ene Castel <sup>1,2,3,8,\*</sup> 

- <sup>1</sup> Normandie University, UNIROUEN, INSERM, U1239 DC2N, 76000 Rouen, France; celeste.nicola2@univ-rouen.fr (C.N.); martine.dubois@univ-rouen.fr (M.D.); campart.cynthia@gmail.com (C.C.); tareq.al-sagheer@univ-rouen.fr (T.A.S.); laurence.desrues@univ-rouen.fr (L.D.)
  - <sup>2</sup> Institute for Research and Innovation in Biomedicine (IRIB), 76000 Rouen, France; damien.schapman@univ-rouen.fr (D.S.); ludovic.galas@univ-rouen.fr (L.G.)
  - <sup>3</sup> Cancer and Cognition Platform, Ligue Nationale contre le Cancer, 14000 Caen, France; m.lange@baclesse.fr (M.L.); F.JOLY@baclesse.fr (F.J.)
  - <sup>4</sup> Normandie University, UNIROUEN, INSERM, PRIMACEN, 76000 Rouen, France
  - <sup>5</sup> Centre Fran ois Baclesse, Clinical Research Department, 14000 Caen, France
  - <sup>6</sup> Normandie University, UNICAEN, INSERM, U1086 ANTICIPE, 14000 Caen, France
  - <sup>7</sup> University Hospital of Caen, 14000 Caen, France
  - <sup>8</sup> Normandie University, UNIROUEN, INSERM, DC2N, Team Astrocyte and Vascular Niche, Place Emile Blondel, CEDEX, 76821 Mont-Saint-Aignan, France
- \* Correspondence: helene.castel@univ-rouen.fr; Tel.: +33-2-35-14-66-23  
† These authors contributed equally to this work.



**Citation:** Nicola, C.; Dubois, M.; Campart, C.; Al Sagheer, T.; Desrues, L.; Schapman, D.; Galas, L.; Lange, M.; Joly, F.; Castel, H. The Prostate Cancer Therapy Enzalutamide Compared with Abiraterone Acetate/Prednisone Impacts Motivation for Exploration, Spatial Learning and Alters Dopaminergic Transmission in Aged Castrated Mice. *Cancers* **2021**, *13*, 3518. <https://doi.org/10.3390/cancers13143518>

Academic Editor: Elizabeth Williams

Received: 2 April 2021

Accepted: 8 July 2021

Published: 14 July 2021

**Publisher's Note:** MDPI stays neutral with regard to jurisdictional claims in published maps and institutional affiliations.



**Copyright:**   2021 by the authors. Licensee MDPI, Basel, Switzerland. This article is an open access article distributed under the terms and conditions of the Creative Commons Attribution (CC BY) license (<https://creativecommons.org/licenses/by/4.0/>).

**Simple Summary:** Cognitive side effects and fatigue after cancer treatment now constitute a major challenge in oncology. Abiraterone acetate plus prednisone (AAP) and enzalutamide (ENZ) are next-generation therapies improving metastatic castration-resistant prostate cancer (mCRPC) patient survival, but also associated with neurological disturbances. We developed a behavioral 17 months-aged and castrated mouse model receiving AAP or ENZ for 5 days per week for six weeks. We establish that ENZ impacts locomotor and explorative behaviors, and strength capacity likely by preventing binding of central synthesized androgens to androgen receptors expressed by dopamine neurons of the Substantia Nigra and the Ventral Tegmentum. ENZ also reduces the cognitive score, associated with less neuronal activity in dorsal hippocampal areas. This demonstrates ENZ-specific consequences on motivation to exploration and cognition, being of particular importance for future management of elderly prostate cancer patients and their quality of life.

**Abstract:** Cognitive side effects after cancer treatment threatening quality of life (QoL) constitute a major challenge in oncology. Abiraterone acetate plus prednisone (AAP) and enzalutamide (ENZ) are examples of next-generation therapy (NGT) administered to metastatic castration-resistant prostate cancer (mCRPC) patients. NGT significantly improved mCRPC overall survival but neurological side effects such as fatigue and cognitive impairment were reported. We developed a behavioral 17 months-aged and castrated mouse model receiving per os AAP or ENZ for 5 days per week for six consecutive weeks. ENZ exposure reduced spontaneous activity and exploratory behavior associated with a decreased tyrosine hydroxylase (TH)-dopaminergic activity in the substantia nigra pars compacta and the ventral tegmental area. A decrease in TH<sup>+</sup>-DA afferent fibers and Phospho-DARPP32-related dopaminergic neuronal activities in the striatum and the ventral hippocampus highlighted ENZ-induced dopaminergic regulation within the nigrostriatal and mesolimbocortical pathways. ENZ and AAP treatments did not substantially modify spatial learning and memory performances, but ENZ led to a thigmotaxis behavior impacting the cognitive score, and reduced c-fos-related activity of NeuN<sup>+</sup>-neurons in the dorsal hippocampus. The consequences of the mCRPC

treatment ENZ on aged castrated mouse motivation to exploration and cognition should make reconsider management strategy of elderly prostate cancer patients.

**Keywords:** metastatic resistant prostate cancer; enzalutamide; abiraterone acetate/prednisone; aged castrated mice; behavior; dopaminergic pathways

## 1. Introduction

It is now accepted that cancer treatments including brain irradiation and/or systemic chemotherapy induce cognitive dysfunctions including learning, memory, information processing speed and executive functions associated with brain structural and functional altered activity [1–3], all referred to as “cancer related-cognitive impairment” or CRCI [4,5]. Long-term CRCI now constitutes a challenge for patients/survivors of localized non-central nervous system (CNS) tumors and may also be associated with targeted therapy such as those involving anti-angiogenic agents [6], novel immunotherapy [7] as well as new generation hormone therapy NGT [6–9]. Currently, the understanding of vulnerability factors of CRCI, most deleterious new cancer drugs and of biological–physiological mechanisms affecting patient neurological functions, fatigue or mood disorders represents important issues in terms of survival and quality of life (QoL) in particular in elderly cancer patients.

Prostate cancer (PC) is a major public health concern, being the second most common cancer among the leading causes of cancer-related death in men in the US/European occidental countries [10,11], and represents the most frequent cancer in the elderly population. In the case of radical prostatectomy and/or radiation therapy following biochemical recurrence, a pharmacological androgen deprivation therapy (ADT) to abolish the gonadal testosterone (T) synthesis is proposed [12]. When progression to metastatic castration-resistant prostate cancer (mCRPC) appears inevitable [13], NGTs are now proposed to this older patient population [14]. One consists of targeting the extragonadal and intratumoral cytochrome P450-17 (CYP17A1) enzyme activity converting pregnenolone and progesterone into T precursors, by abiraterone acetate, a prodrug of abiraterone, in association with prednisone (AAP), to avoid cortisol deficiency [14]. The other strategy consists in the next generation of androgen receptor (AR) irreversible high-affinity antagonist enzalutamide (ENZ), impairing AR translocation to the nucleus and interaction with DNA androgen-response elements [15,16]. These treatments significantly improve the overall survival (OS) of patients with mCRPC before or after chemotherapy [14,17–19]. For now, in the absence of better mCRPC therapy, the relative efficacy associated with good tolerability profile of AAP and ENZ [20] tends to increase their availability to elderly patients [21]. Because aging by itself is associated with functional decline, this population of cancer patients appears at greater risk for increased age-related brain changes secondary to cancer and cancer treatments [22] impacting QoL. Interestingly, delayed health-related QoL alteration and pain progression was observed for ENZ or AA compared with chemotherapy [15,23,24], but their impact has never been evaluated in mCRPC patients on objective cognitive functions, despite a current clinical trial [21]. Recently, neurological events were described with ENZ [25], confirmed in a prospective phase IV study showing more fatigue and subjective cognitive impairments in ENZ- than in AAP-treated mCRPC patients [26]. These symptoms may be explained by central production of T and dihydrotestosterone (DHT) via peripheral steroid intermediates metabolism or de novo central synthesis by steroidogenic enzymes [27,28], expressed in different brain areas [29] including hippocampal CA1-CA3 and dentate gyrus (DG) in rodent brain [30,31]. Together, NGT may impact brain functioning and induce fatigue related to QoL, as well as cognitive impairment in mCRPC elderly vulnerable patients.

The study herein aims at dissecting the direct brain impact of NGT in the context of aging and androgen deprivation in a behavioral preclinical model of aged castrated male mice. We explored the impact of oral treatment of ENZ or AAP on spontaneous activity,

emotional reactivity including anxiety- and depressive-like behaviors, as well as spatial and learning memory. We found that ENZ exposure reduces spontaneous activity and exploratory behavior and impairs dopamine (DA) neurons of the substantia nigra pars compacta (SNpc) and the ventral tegmental area (VTA), leading to reduced DA production throughout nigrostriatal and mesolimbocortical pathways. Additionally, neither ENZ nor AAP treatments drastically altered spatial learning, memory and behavioral flexibility, but ENZ led to deficits in spatial cognitive strategies and to a decreased dorsal hippocampal (dHP) neuronal activity.

## 2. Materials and Methods

### 2.1. Animal Housing and Management

57Bl/6J Rj male mice of 15 months old were surgically castrated under the following institutional animal care and European guideline within the Janvier laboratory (Le Genest-Saint-Isle, France) following a conventional protocol. In anesthetized mice, the surgical area was aseptically treated, the peritoneum incised and the left or right testicular fat pad holding the testis were gripped and cut using a sterile scalpel. After cauterization of the testicular artery, the peritoneum is sutured, the skin is stapled with surgical wound clips and analgesia is performed to manage pain (carried by Janvier Laboratories (Le Genest-Saint-Isles, France)). At the age of 17 months, castrated mice were delivered to our institute animal facility. Mice were group-housed under controlled standard environmental conditions:  $22 \pm 1$  °C, under an inverse 12/12 h light/dark cycle (light on: 00:00 to 12:00), with water and food available ad libitum. After 2 weeks of adaptation, animals were daily handled for weight monitoring for 1 week, and then throughout the treatment period. Treatment administration began at 17 months and 2 weeks of age while entire experimental sessions run for 6 additional weeks. The behavioral tests were performed during the active phase of mice (from 01:00 PM). For some control experiments, control aged non-castrated mice were also obtained from Janvier Labs and tested at 18 months and 2 weeks aged on some behavioral tasks. All mice were euthanized at 19 months. The number and the suffering of animals were minimized in accordance with the guidelines of the European Parliament and Council Directive (2010/63/EU) and the Council for the Protection of Animals Used for Scientific Purposes. This project was approved by the “Comité d’Ethique Normandie en Matière d’Expérimentation Animale” and the French Research Minister (#7866-2016112115226170 v5) and carried out under the supervision of authorized operators (H.C. and M.D.).

### 2.2. Treatment Administration

For chronic treatments, mice received per os vehicle or NGT every day for 5 days per week for six consecutive weeks. An amount of 100  $\mu$ L/10 g/day of vehicle of ENZ (Veh-ENZ): 1% CMC (carboxymethylcellulose sodium), 1% tween 80, 5% dimethyl sulfoxide (DMSO) (Sigma Aldrich, Saint-Quentin-Fallavier, France) or ENZ (MedChem Express, Monmouth Junction, NJ, USA): 30 mg/kg in Veh-ENZ, the vehicle of abiraterone acetate (Veh-AAP): 20% hydroxypropyl  $\beta$  cyclodextrine (Hp $\beta$ CD), 0.037N HCl, 0.13 $\times$  PBS in dH<sub>2</sub>O (Sigma-Aldrich) or abiraterone acetate-prednisone (AAP): 200 mg/kg of abiraterone acetate (Janssen Research and Development, Issy-les-Moulineaux, France) + 500  $\mu$ g/kg prednisone (Sigma-Aldrich) Veh-AAP, every day for 5 days per week for six consecutive weeks. The treatments were administered per os with 22G feeding needles (Fine Science Tools, Heidelberg, Germany). Concerning the experimental session of Veh-AAP and AAP administration, food deprivation was done for all mice 2 h before and 1 h after treatment because the composition of meals can affect AAP pharmacokinetic. Aged control mice were non-castrated, did not receive oral administration of vehicle or treatment.

### 2.3. Behavioral Tests

Behavioral test panels were selected to evaluate the impact of the castration process (aged control mice, qualitative observational study) and of the treatment with ENZ or AAP

versus vehicles on activity and exploration, emotional reactivity and cognitive functions. Thus, as soon as received, animals were distributed at random in the different experimental groups, at a rate of 5 mice per cage. All tests were performed as previously described [5] with slight modifications. The spontaneous activity and exploration of animals were evaluated in the open-field test (OFT). Anxious-like behaviors were assessed by means of the elevated plus maze (EPM) and the light and dark emergence test (LDB). Depressive-like behaviors were evaluated with the tail suspension test (TST) and the forced swim test (FST). Then, spatial learning, spatial memory as well as behavioral flexibility were measured in the Morris water maze (MWM). In total, 5 behavioral experimental sessions were conducted. At the end of experimental sessions, brains and blood samples were collected from each group to lead immunohistochemical experiments on CNS slices and quantification of cytokine and hormones from plasma collection, respectively.

#### 2.4. Open Field Test

The general activity was measured for 10 min by placing mice in an OFT apparatus ( $45 \times 45 \times 31 \text{ cm}^3$ , LxH). The OFT is a widely used device measuring exploratory and locomotion activity in a novel environment, a dopamine-dependent process [32]. The animal was placed into the center of the apparatus and several behavioral parameters (distance crossed, vertical activity and grooming) were automatically analyzed by the videotracking system Anymaze (Stoelting<sup>®</sup>, Dublin, Ireland). Rodents typically prefer not to be in the center, lit area of the apparatus and tend to walk close to the walls (thigmotaxis) since this is a novel, and presumably, stressful, environment to the animal. So distance and time spent in the center part of the device is an indication of anxiety [33], but motor activity and exploration can also provide a behavioral incentive value [34].

#### 2.5. Elevated Plus-Maze

Anxious-like behaviors were evaluated by means of the EPM in a unique session of 5 min as previously described to evaluate state anxiety (i.e., in a forced situation) [35] and by LDB (supplementary information). It allows determining emotional reactivity of animals through a conflict between secure parts of the maze (2 enclosed arms) and aversive parts of the maze (2 open arms) of a device elevated at 41.5 cm above the floor. Time spent and number of entries into the open and enclosed arms of the maze were measured and the percent number of entries and percent time in open arms were calculated.

#### 2.6. Tail Suspension Test and Forced Swim Test

Depressive-like behaviors were evaluated in the TST [36] or the FST [37], two standard procedures used to evaluate the antidepressant activity of pharmacological compounds. In TST, mice were suspended at a height of 20 cm above the floor and are surrounded by an enclosure and the total duration of immobility (passive hanging) between periods of wriggling to avoid aversive situation was measured for a period of 6 min, and the latency to the first immobility was also noted, as previously described [38]. In FST, mice were placed for 6 min into a cylinder (17 cm in diameter) filled with 25 °C tap water (at a height of 13 cm) with no way out. The immobility duration (excluding movement necessary to keep the head above water or to float) was measured as an indication of the behavioral despair of mice [38].

#### 2.7. Morris Water Maze

Spatial learning and memory performances, as well as learning plasticity, were evaluated in the MWM [38,39] as previously described. Briefly, mice were placed in a water tank and had to escape water by finding a hidden platform (9.7 cm in diameter). Behavior of animals was videotracked with Anymaze (Stoelting<sup>®</sup>, Dublin, Ireland). Tests were conducted in several sessions [38], each session being composed of 4 trials of 60 s maximum each (except the probe test). The first session (familiarization) was conducted by placing the escape platform in the center of the pool. Mice were placed on it for 20 s and immediately

after, the mice were placed in water, facing the wall, at one of the 4 starting points (East, E; North, N, West, W; south, S) for a trial of maximum 60 s. If mice did not find the escape platform within the 60 s maximum duration of trial, animals were manually placed on it for 20 s. Then 3 successive trials, with intertrial intervals of 30 min, were conducted with a departure from one of the 3 other starting points. In the 4 consecutive days, the spatial learning abilities were tested by placing the escape platform in the NW quadrant. Animals had to use the distal visual cues around the basin to find the platform location. Each day, 4 trials of 60 s maximum were conducted. On the 4th day of the hidden platform phase, 2 h after the end of the 4th trial, a probe test was conducted by removing the platform and allowing animals to swim into the pool for a unique trial of 60 s. Time spent by mice in the previously correct quadrant (NW) was measured. Spatial memory abilities were evaluated on the 3rd day, during the retrieval test. The platform was hidden in the NW quadrant and mice had a maximum of 60 s to find its location, for four successive trials for a unique day. On the 9th day, the platform was moved from the NW to the SE quadrant and behavioral flexibility was studied and the procedure was the same as previously described for the hidden platform test.

### *2.8. Swim Search Strategy Analysis, Dataset Preparation and Cognitive Score from MWM*

In MWM spatial learning session, trial after trial, the animals accumulate knowledge of the spatial relations of the cues and the specific contexts allowing effective navigating routes to find the hidden platform. Stereotypic sequences of search patterns with swim path trajectories can be analyzed as they can be considered representative of cognitive functions during the task. Graziano et al. [40], put forward automatization of several explorative strategies. Here, as previously established [41], image files corresponding to tracking trajectories for each mouse in all trials along the 4 consecutive training days were obtained (AnyMaze; Stoelting Co., Wood Dale, IL, USA) and manually labelled according to the 6 categories of trajectories as previously described [41]: thigmotaxis, scanning, circling, focal search, rotating and direct swim. If some traits were mixed within one trial, most prominent trajectory was adopted as label. Representative trajectories are shown as previously described [41], a convolutional neural network (CNN) with two convolution layers were used to classify the swim path trajectories, by means of the minimal available program from the repository (<https://figshare.com/s/90d7b2d038551efe08ec>; accessed on 26 April 2020) [41] which help us designing our study model. In this work, recognition model output was then used to assign each image to the respective subset. For the model construction, swim path images of familiarization, retrieval and flexibility phases were collected for each mouse group from AnyMaze (Stoelting®, Dublin, Ireland). The dataset (420 images) was divided into two sub-datasets; 80% of the data were used for the training stage and the other 20% were used for validation. In this model proposed by Higaki et al. [41], we integrated new instructions to create an unbiased automatic tool able to recognize unlabelled images. Thus, unlabelled swim path images of the learning phase were collected and randomly passed in our modified model. The original format was a Microsoft Windows Bitmap Image (BMP) file with  $140 \times 120$  pixel size and 32-bit color data. All image data were converted to grayscale pictures of reduced pixel size ( $48 \times 48$ ) using a free image processing tool of Python interpreter (Pillow; Alex Clark and Contributors). As previously [41], pixel values derived from each image file were divided by 255 for standardization and passed to our modified CNM as input data. Whole image files were randomly rearranged before being assigned to each subdataset. Repeated holdout cross-validation was performed 5 times for each randomly rearranged dataset, and the average score was employed as the valid outcome. All these modeling processes were provided by Chainer, previously validated for this procedure [41,42]. In addition, we built a score corresponding to cognitive performance in each training trial as previously described [41,43], attributing a higher score to the best efficient cognitive strategy: Thigmotaxis: 0, Scanning: 1, Circling: 2, Focal search: 3, Rotating: 4, Direct

swim: 5. Average cognitive score within 4 trials and for 4 learning days in each mouse was calculated and used for the analysis.

### 2.9. Brain Analyses

At the end of the treatment sessions, mice were subjected to intraperitoneal injections of BrdU (5-bromo-2-deoxyuridine, Sigma-Aldrich) at 50 mg/kg once a day for 4 days to label adult-generated progenitor cells in the DG of the hippocampus. Thus, proliferation of BrdU<sup>+</sup>-precursors and dopaminergic activity in the SNpc and VTA and consequences via afferences in the striatum and ventral hippocampus were investigated by immunohistochemistry on brain slices. After the last injection of BrdU on the fourth day, mice were anesthetized using isoflurane (Isovet, Osalia, Paris, France), decapitated and each brain was immediately removed and frozen in 2-methylbutane (Sigma-Aldrich) at  $-30^{\circ}\text{C}$  and then stored at  $-80^{\circ}\text{C}$  until use. Brain sections (20  $\mu\text{m}$  thick) were cut with cryostat, from the anterior part of the dorsal hippocampus (anteroposterior, 1.08 mm from the Bregma  $-1.46$  mm). Every 12th section, each separated by 240  $\mu\text{m}$ , was mounted on slides coated with gelatin-chrome alum (VWR International, Leuven, Belgium) and stored at  $-20^{\circ}\text{C}$  until processing. Eight hippocampal sections from 3 to 4 animals per group were stained simultaneously for immunohistochemical observations and quantifications. Slices were post-fixed with formaldehyde (4%, Sigma-Aldrich) for 15 min at  $4^{\circ}\text{C}$ , rinsed in PBS (0.1 M, pH 7.4, Sigma-Aldrich), permeabilized with X-100 triton (Fisher Scientific, Illkirch, France) 0.05% and non-specific binding sites were blocked with a permeabilization/blocking solution containing PBS (Sigma-Aldrich), 0.5% BSA (Roche, Mannheim, Germany), 0.1% X-100 triton and 10% NDS (Normal Donkey Serum, Sigma-Aldrich) for 60 min at room temperature (RT). For BrdU immunostaining, brain slices were first incubated in a 2N-HCl for 45 min at  $45^{\circ}\text{C}$  and then rinsed in a boric acid (Sigma-Aldrich) solution 0.1 M at pH = 8.5 for 10 min. Brain slices were incubated overnight (12h) at  $4^{\circ}\text{C}$  with the primary antibodies of interest diluted in the permeabilizing/blocking buffer (PBS, 0.5% BSA, 0.1% X-100 triton and 1% NDS). The following primary antibodies and the corresponding dilutions were used as followed: anti-GFAP (Goat, Abcam, Cambridge, UK, AB53554, 1:1000) or anti-GFAP (Rabbit, Dako, Agilent, Santa Clara, CA, USA, Z0334), anti-AR (Rabbit, Abcam AB74272, 1:300), anti-BDNF (Goat, St John's Lab, London, UK, STJ73299, 1:1000), anti-TH (Goat, Abcam AB101853) or anti-TH (chicken, Abcam AB76442, 1:500), anti-Phospho-DARPP-32 (P-DARPP-32, Rabbit, Bioss, Boston, MA, USA, bs-3118R, 1:200), anti-BrdU (Sheep, Abcam AB1893, 1:200), anti-NeuN (Rabbit, Abcam AB104225) or anti-NeuN (Chicken, MyBiosource MBS837654, 1:1000), anti-c-fos (Rabbit, Abcam AB190289), anti-DCX (Guinea pig, Millipore, Burlington, MA, USA), anti-D1R (Rabbit, Abcam, AB20066, 1:200) or anti-CYP17A1 (Rabbit, LifeSpan Biosciences Inc., Seattle, WA, USA, LS-C352100, 1:100). The following day, sections were rinsed (PBS,  $4 \times 5$  min) and incubated (2h, RT) with the appropriate secondary Alexa Fluor-conjugated antibodies diluted in the permeabilizing/blocking buffer (2h, RT). Secondary antibodies were used as followed: Alexa 647-donkey anti-goat (Abcam AB150131, 1:1000), Alexa 488-donkey anti-rabbit (Invitrogen, Carlsbad, CA, USA, A21206, 1:1000), Alexa 488-donkey anti-sheep (Invitrogen A11015, 1:1000), Alexa 488-donkey anti-rat (Invitrogen A31573, 1:1000), Alexa goat anti-guinea pig (Invitrogen A11073, 1:1000) and Alexa 488-goat anti-chicken (Abcam, AB150173). Sections were then rinsed with PBS ( $3 \times 5$  min at RT) and then cell nuclei were stained with a DAPI solution (Sigma-Aldrich, 1  $\mu\text{g}/\text{mL}$ ) incubated for 5 min at RT. Slices were embedded in a Mowiol solution, dried overnight at RT, and then stored at  $4^{\circ}\text{C}$  until they were observed with an epifluorescence microscope (PRIMACEN, upright microscope Nikon 1, Nikon, Champigny/marne, France) as first evaluation, and by confocal microscopy (PRIMACEN, Upright confocal microscope, Leica Microsystems, Nanterre, France) for image acquisition and quantification. Labeled structures were assessed in 4 sections of 20  $\mu\text{m}$  thickness (anteroposterior from bregma 0.62 mm, interaural 4.42 mm for striatum, at bregma  $-1.82$  mm, interaural 1.98 mm for dorsal hippocampus (dHP), at bregma  $-3.16$  mm, interaural 0.64 mm for ventral hippocampus (vHP) at bregma  $-3.08$  mm, interaural 0.72 mm for the substantia nigra pars compacta

(SNpc) and ventral tegmental area (VTA) with SP8 confocal microscope (Leica, Heidelberg, Germany). The density, fluorescence intensity and total number of cells were quantified by using Image J software (version 1.8.0, NIH, USA).

### 2.10. Statistical Analysis

Prior to analysis, each treatment group normality was checked by Shapiro–Wilk normality tests, and variances were analyzed. The potential existence of outliers was verified thanks to the Grubs test. Based on the groups' normality and analysis of variances, data were analyzed using either (i) two-way ANOVA followed by Sidak's multiple comparisons test or t-test for parametric analysis, or (ii) Kruskal–Wallis followed by Dunn's multiple comparison test or Mann–Whitney test for non-parametric analysis. For the analysis of swim path strategies in the Morris water maze, chi-square test ( $\chi^2$  test) with Yates' continuity correction was used (Confidence interval 95%). For cognitive score analysis, statistical analysis was performed by repeated measures (RM) one-way ANOVA, both using the Tukey's test for multiple comparisons. For all analyses, a  $p$ -value  $\leq 0.05$  was considered significant. Elisa quantifications were performed from 6 to 9 plasma samples of each group. For immunohistochemistry analysis, based on groups normality and equivariance, data were analyzed using either (i) Mann–Whitney test for non-parametric analysis, or (ii) unpaired t-test for parametric analysis. For all analyses, a  $p$ -value  $\leq 0.05$  was considered significant. Data are expressed as scatterplots and mean  $\pm$  Standard Error of the Mean (SEM) and analyzed using GraphPad Prism-7 software (La Jolla, CA, USA).

## 3. Results

We explored for the first time the neurological impact of NGT in aged castrated mice to model a clinical situation encountered by mCRPC patients first treated via ADT and then receiving either ENZ or AAP (Figure 1A). Our work is mainly focused on the potential regulatory mechanisms of ENZ or abiraterone (AA), blocking the enzymatic activity of CYP17A1 in adrenal glands (and prostate) but also within some brain areas (Figure 1A). We chronically administered 100  $\mu$ L/10 g of ENZ or AAP per os for 6 weeks to 17.5 months old C57BL/6 male mice, castrated at 15 months old to mimic ADT. This model is based on the assumption that CYP17A1 expressed in brain structures is likely responsible for the conversion of pregnenolone and progesterone towards T and potentially DHT on one hand, and in estrogens on the other hand (Figure 1B). This local androgen production may control AR-activating signaling pathways in selective brain areas, regulating aged mouse neurobehavioral responses in the context of androgen deprivation.

### 3.1. ENZ but Not AAP Treatment Reduced Spontaneous Activity, Exploration and Motivation to Effort with No Impact on Plasma Cytokines

We evaluated the behavioral consequences of per os ENZ or AAP treatment for 5 consecutive days for 6 weeks, on general spontaneous activity and exploration, emotional reactivity and spatial learning and memory in aged castrated mice by means of validated behavioral tests (Figure 2A). No significant effect of ENZ or AAP was detected on the course of weight gain (Figure S1). Based on the findings that low levels of T in men can be associated with inflammatory status in different situations such as in healthy elderly population [44,45] or hypogonadism [46], common cytokines were measured in plasma of aged castrated mice and non-castrated/non treated mice. We did not show a significant difference in the pro-inflammatory, pluripotent, chemotactic or anti-inflammatory cytokine levels between ENZ or AAP and their vehicle groups, and the control group (Table S1), discarding a potential consequence of NGT on systemic cytokine modifications in aged subjects.

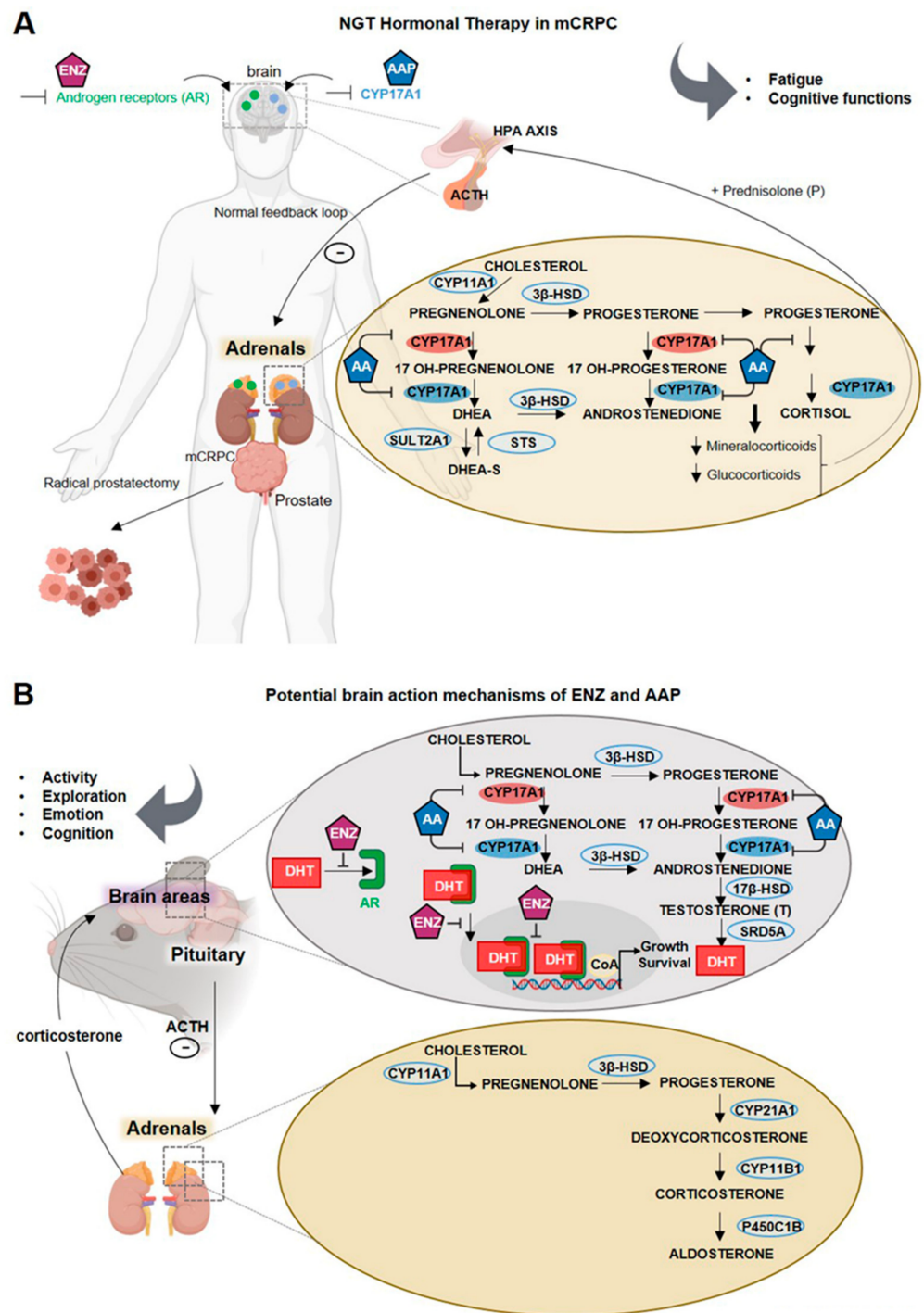


**Figure 1.** New generation therapy targeting androgen biosynthesis in addition to androgen deprivation therapy against metastatic castration-resistant prostate cancer: potential mechanisms of action on brain function using a mouse model. Note. (A) Schematic of enzalutamide (ENZ) and abiraterone acetate-prednisone (AAP) as treatment options for metastatic castration-resistant prostate cancer patients and of their sites of action such as prostate tissue, adrenals and potentially the brain. Cytochrome p450c17A1 (CYP17A1), an ER-localized enzyme expressed in both prostate and adrenal glands, and potentially in the human brain, plays a critical role in the androgen biosynthesis pathway. In the adrenals, CYP17A1 catalyzes two critical steps through its 17 $\alpha$ -hydroxylase and C17,20-lyase activities. The 17 $\alpha$ -hydroxylase activity of CYP17A1 converts pregnenolone to 17 $\alpha$ -pregnenolone and progesterone to 17 $\alpha$ -progesterone. The C17,20-lyase activity of CYP17A1 converts 17 $\alpha$ -hydroxypregnenolone to dehydroepiandrosterone (DHEA) and 17 $\alpha$ -hydroxyprogesterone to



androstenedione, which are subsequently converted to testosterone and/or 5 $\alpha$ -dihydrotestosterone (DHT) by other steroidogenic enzymes. After radical prostatectomy and androgen deprivation therapy, androgens can be mainly synthesized from cholesterol through multiple enzymatic reactions within adrenals. Abiraterone is a novel CYP17A1 inhibitor that acts to inhibit its 17 $\alpha$ -hydroxylase and/or C17,20-lyase activities. To ensure a normal mineralocorticoid feedback loop, low doses of prednisone are co-administered with AA in order to suppress ACTH, thereby restoring normal cortisol physiology in patients. ENZ is an irreversible antagonist with high affinity for the AR expressed both in adrenal glands and also within the brain. **(B)** NGT Hormonal therapy potential action mechanisms on the mouse brain. Representation of ENZ and AAP potential action mechanism in castrated mice illustrating the potential binding of ENZ on AR in the rodent adrenals but also in the brain or the inhibitory action of AAP on CYP17A1 expressed in adrenals and in rodent brain. AA may impact steroidogenesis within adrenals showing the cholesterol transformation into pregnenolone by Cytochrome P450 Family 11 Subfamily A Member 1 (CYP11A1), being metabolized by 3 $\beta$ -hydroxysteroid dehydrogenase (3 $\beta$ -HSD) into progesterone. Through multiple enzymatic reactions within adrenals, progesterone will be transformed in the mineralocorticoid aldosterone. In the upper panel, representative scheme of the steroidogenesis within CNS showing the cholesterol transformation into pregnenolone by Cytochrome P450 Family 11 Subfamily A Member 1 (CYP11A1) in the inner mitochondrial membrane, being metabolized by 3 $\beta$ -hydroxysteroid dehydrogenase (3 $\beta$ -HSD) into progesterone. AAP, by blocking CYP17A1, may impair progesterone transformation into 17-OH-progesterone, 17-OH pregnenolone and Dehydroepiandrosterone (DHEA) as well as transformation of DHEA into androstenedione by 3 $\beta$ -HSD, transformation of androstenedione to testosterone by the 17 $\beta$ -hydroxysteroid dehydrogenase (17 $\beta$ -HSD) and reduction of T to DHT by 5 $\alpha$ -reductase (SRD5A). ENZ treatment potentially impairs the binding of T/DHT to AR, the translocation of ligand-activated-AR into the nucleus and its action as a transcription factor when associated with the coenzyme A (CoA). Modulation of AR signaling transduction activated by local synthesis of T or DHT, should thus regulate neurotransmission, neurogenesis, and brain plasticity and selective behavioral responses as activity, emotion, exploration or cognitive functions. 17 $\beta$ -HSD, 17 $\beta$ -hydroxysteroid dehydrogenase; 3 $\beta$ -HSD, 3 $\beta$ -hydroxysteroid dehydrogenase; AAP, abiraterone acetate-prednisone; ACTH, Adrenocorticotrophic hormone; AR, androgen receptor; CNS, central nervous system; CoA, coenzyme A; CYP11A1, Cytochrome P450 Family 11 Subfamily A Member 1; CYP17A1, cytochrome P450 family 17 subfamily A member 17; DHEA, dehydroepiandrosterone; DHT, dihydrotestosterone; ENZ, enzalutamide; ER, estrogen receptor; NGT, new generation hormone therapy; SRD5A, 5 $\alpha$ -reductase.

The impact of ENZ and AAP was tested by using behavioral paradigms for spontaneous activity and exploration in a new environment, anxiety, depressive-like behavior involving motivation to effort, all validated in non-castrated aged mice (Table S2). In OFT, ENZ-treated compared with Veh-ENZ groups showed a significant increase in time spent immobile, and a decrease in the number of vertical episodes, center entries and distance crossed (Figure 2B and Table S3), suggesting a reduction of locomotion for exploration. In contrast, AAP- and Veh-AAP-treated mice exhibited normal activity, locomotion and exploration, and no group effect was observed for main parameters, except a decreased grooming time (Table S3), suggesting reduced arousal in an aversive/stressing environment. Because mice exposed to EPM and LDB tests showed no alterations after ENZ or AAP compared with Vehicle treatments (Table S3), even if AAP was associated with more head dips (Table S3), it appears that anxiety-like behaviors are not worsened with NGT. To verify depressive-like behavior and/or lack of sustained expenditure to effort, the resignation was assessed by presenting rodents FST and TST. In FST, neither ENZ- nor AAP-treated groups exhibited significant changes in immobility duration and latency to the first immobile episode (Figure 2C) compared with Veh-treated groups. However, in TST, ENZ mice exhibited an increase of time spent immobile compared with Veh-ENZ (Figure 2C), while no differences were detected in AAP compared with Veh-AAP mice (Table S3).

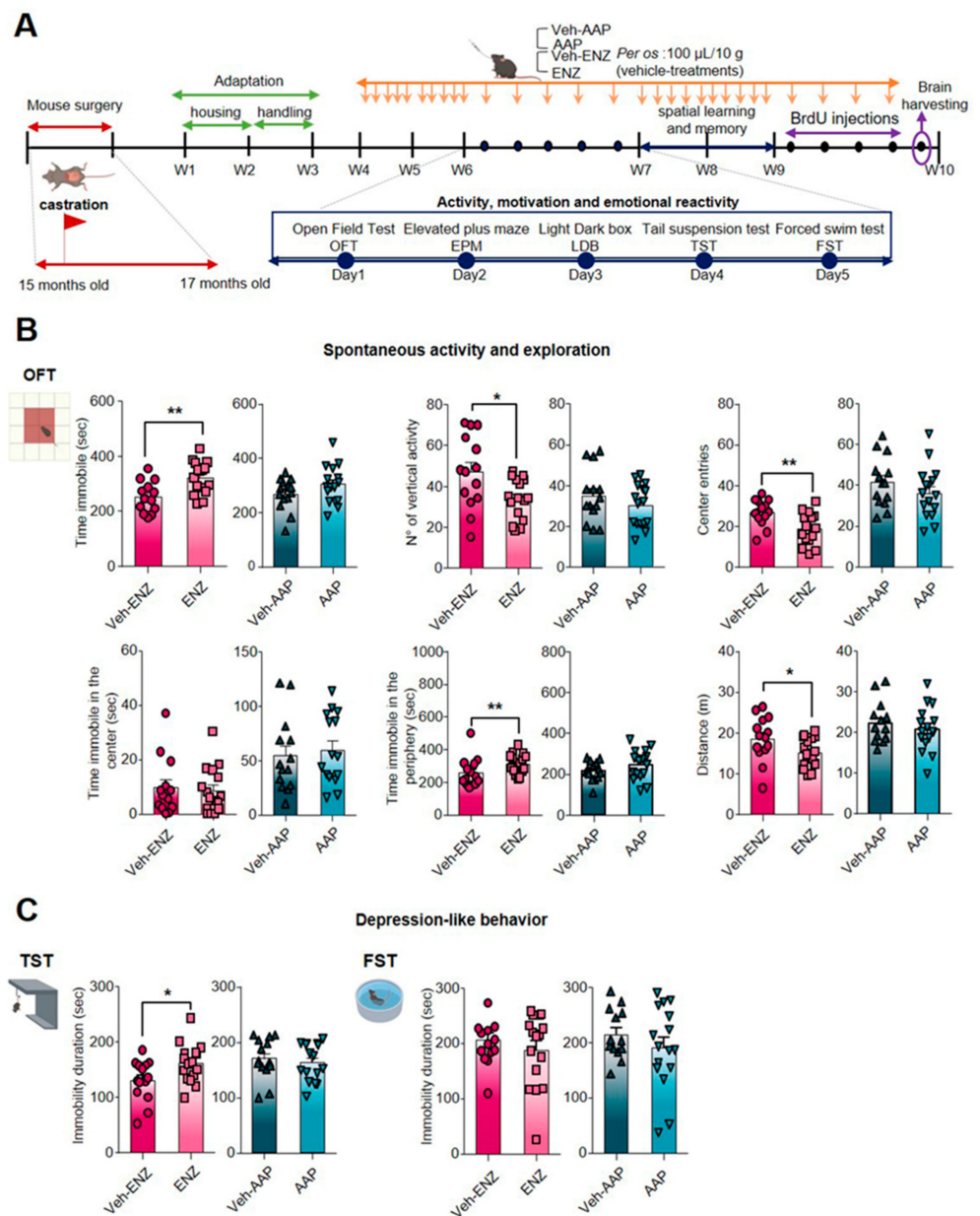


**Figure 2.** Characterization of ENZ or AAP impact on incentive exploratory behavior and motivation to the effort of mice. Note. (A) Schematic diagram showing the timeline for treatments and behavior experiments for ENZ and AAP treatments. Note. C57BL/6J Rj mice were castrated at 15 months old, were housed under controlled environment from 17 months old, while treatments were administered orally (per os) once a day for five per week, from week 4 (W4) to week 10 (W10), as indicated (orange arrow). Behavioral evaluations (blue arrow) started at W6, using an open-field test (OFT) on D1, elevated plus maze (EPM) on D2, light-dark box (LDB) on D3, tail suspension test (TST) on D4 and forced swim test (FST) D5. Mice brain and plasma were collected (purple arrows) at the end of W10 after the cognitive evaluation session. (B,C) Impact of ENZ or AAP compared with vehicle on spontaneous activity and exploration in OFT and on resigned behavior/motivation to effort in TST (left) and FST (right panel). Behavioral statistical analyses were performed between vehicle ( $n = 14$ ) and treated ( $n = 16$ ) mice using unpaired t-test or Mann–Whitney test; Bars are mean  $\pm$  SEM while symbols individual data points; \*  $p \leq 0.05$ , \*\*  $p \leq 0.01$ . AAP, abiraterone acetate-prednisone; D, day; ENZ, enzalutamide; EPM, elevated plus maze; FST, forced swim test; LDB, light-dark box; OFT, open-field test; TST, tail suspension test.

### 3.2. ENZ Treatment Altered the Nigrostriatal Network by Inhibiting the Tyrosine Hydroxylase- and Phospho-DARPP32-Related Dopaminergic Activities

Radar plots of Figure 3A highlight that ENZ diminished spontaneous locomotor activity and exploration whereas AAP remained without significant deleterious effects on emotional or spontaneous activity. Dopaminergic pathways have been shown to drive exploratory and locomotion behaviors promoting the positive valuation of novel stimuli as well as motivation to explore [32]. In the rodent brain, DA projections from SNpc to the striatum (Nigrostriatal pathway) are critical for activity or action sequence initiation and performance [47] while DA projections from VTA to the ventral hippocampus (vHP) (part of the mesolimbocortical pathway) are involved in novelty detection and motivation to explore [48,49]. Based on previously published evidence suggesting that AR can be expressed in SNpc and VTA [50,51], we focused here on the consequences of ENZ or AAP treatment on DA-mediating signalings involved in locomotor activity and motivation to exploration (Figure 2A). We analyzed AR expression in DA subpopulations co-stained with an anti-tyrosine hydroxylase (TH) antibody in both SNpc and VTA midbrain nuclei from brain slices of ENZ-, AAP- and Veh-treated groups. AR expression remained constant among the different groups, some neurons being co-stained with TH (Figure 3B). The number of TH+cell/ $\mu\text{m}^2$  appeared significantly diminished in ENZ-treated groups compared with Veh-ENZ in VTA and SNpc, whereas no difference in TH expression level was found between AAP and Veh-AAP conditions (Figure 3D). Importantly, CYP17A1 appeared expressed in both SNpc and VTA areas of ENZ, AAP and respective Veh-treated groups (Figure 3C), indicating that components of local synthesis of T and DHT and of AR signalings are present in the midbrain DA neurons.

### 3.3. ENZ Inhibited the DA-Related P-DARPP-32 Activity in D1R-Expressing Neurons of the Striatum and the Ventral Hippocampus

To verify whether the TH-reduced expression in the SNpc may alter the nigrostriatal DA pathway, the potential diminished DA transmission was tested in regard to the afferent TH-expressing fibers and the co-occurrence of D1R expression with the phospho-DARPP-32 (P-DARPP-32) labeling in the striatum (Figure 4). ENZ, but not AAP, led to the inhibition of the staining intensity of the TH+-fibers when compared with respective vehicles (Figure 4A,B). To assess a potential impact on the DA synaptic transmission, we quantified the labeling of P-DARPP-32 particularly in neurons expressing D1R likely indicative of striatal medium spiny neurons (MSNs) activation. ENZ when compared with Veh-ENZ, drastically and significantly led to inhibition of striatal P-DARPP-32 staining mostly found in NeuN+-neurons while P-DARPP-32 was not modified between AAP- and Veh-AAP-group conditions (Figures 4 and S2). These results suggest that ENZ is associated with a diminution of TH-expression in AR+-neurons in SNpc and striatal DA activity, potentially associated with ENZ-evoked reduced motivation for movement.

VTA activity can be connected to the hippocampus, to the vHP in particular where some projections are dopaminergic [52]. vHP can be involved in limbic functions regulating the impact of emotional experiences [53] and controlling exploration of novelty and motivated behaviors [54]. Here we detected only a modest expression of AR in the DG, as well as in CA1 and CA3 of vHP more specifically in NeuN+-neurons and not GFAP+-glial cells from ENZ-, AAP- and vehicle-treated groups (Figure S3). To examine the impact of ENZ on VTA-dopaminergic projections to vHP neurons, the expressions of TH, P-DARPP-32 and the immediate early gene (c-fos) were quantified. TH+-fibers showed reduced staining intensity in the ENZ compared with Veh-ENZ group while AAP failed to alter TH labelings (Figure 5A). Moreover, in most D1R+-neurons, a decrease in P-DARPP-32+-cells and P-DARPP-32+-neurons (NeuN+-cells) (Figure S4) in the vHP area was found in ENZ-treated brain slices (Figure 5B). This was associated with the repression of cFos+/NeuN+ neuronal cells in the vHP DG, CA3 and CA1 mainly in the ENZ group (Figure 5C). These results suggest that ENZ mainly impairs vHP hippocampal activity by modulation of dopaminergic neuronal stimulation from VTA, even if the contribution of the local inhibition of AR cannot be excluded.

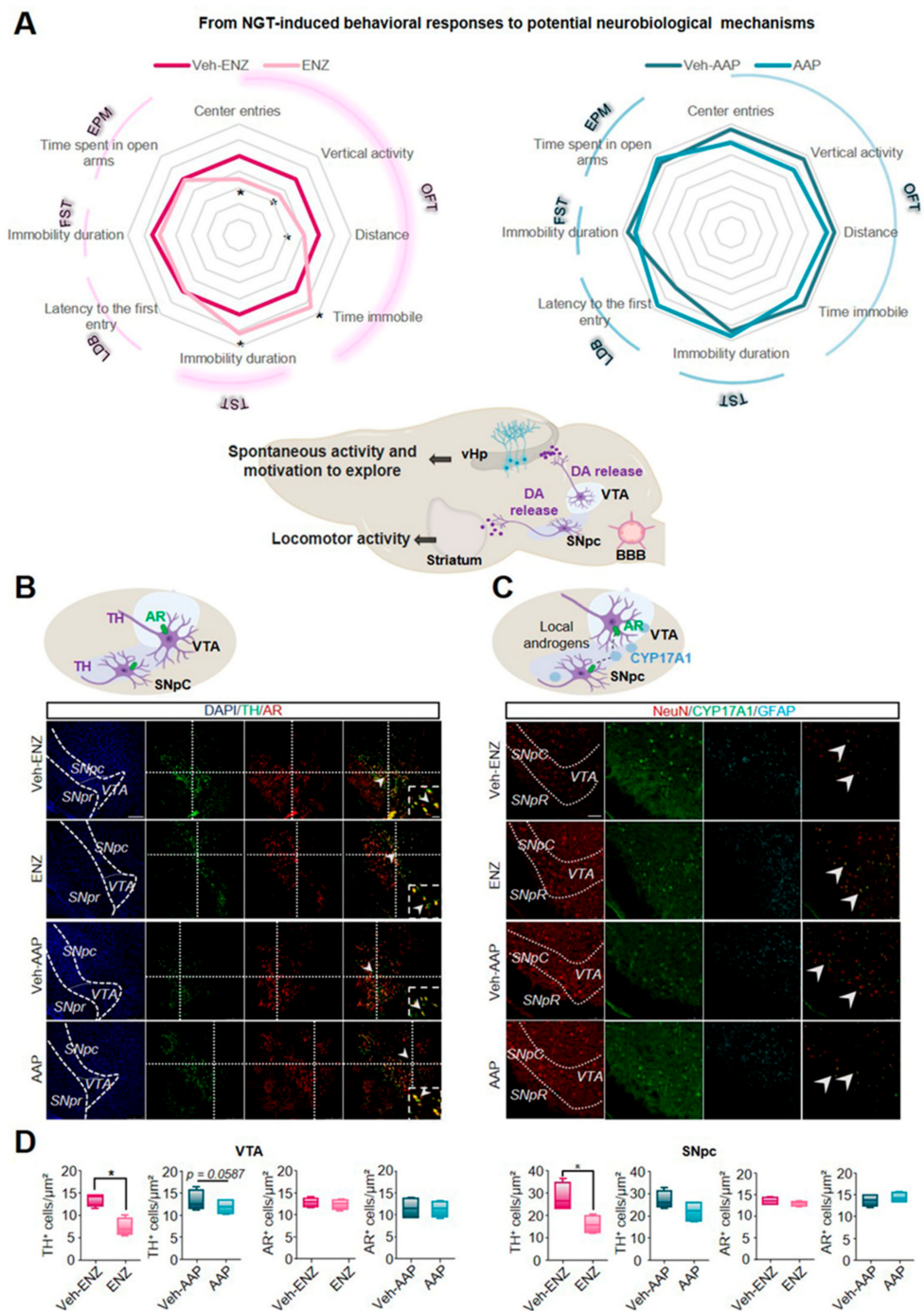


**Figure 3.** AR and CYP17A1 are expressed in the substantia nigra pars compacta and ventral tegmental area and ENZ inhibits dopaminergic activity in both midbrain nuclei. Note. (A) Comparative Radar Chart of performance index scores across emotional and exploratory behavioral domains after ENZ (left panel) or AAP (right panel) treatments compared with Vehicles as presented in Figure 2A and Table S3. Based on the behavioral modifications, schematic representation (Middle panel) of nigrostriatal and corticolimbic circuits potentially involved in ENZ-altered locomotor activity and exploration. Based on previous studies, AR may be expressed in ventral tegmental area (VTA) and substantia nigra pars compacta (SNpc) dopaminergic neurons. SNpc projects dopamine (DA) axons to the striatum (nigrostriatal pathway) while VTA projects DA axons to ventral hippocampus (vHp) (corticolimbic pathway), also expressing AR. Statistical analysis was done on performances of vehicle ( $n = 14$ ) and treated ( $n = 16$ ) mice using unpaired  $t$ -test or Mann–Whitney test; Data are mean  $\pm$  SEM; \*  $p \leq 0.05$ . (B) Schematic drawing of SNpc and VTA dopaminergic neurons expressing AR. Tyrosine

hydroxylase (TH) (green) and AR (red)-immunoreactivity in the SNpc and VTA of ENZ-, AAP- and Vehicle-treated mice. The boxed areas showed magnification of clusters of TH+/AR+ cells. Scale bar: 250  $\mu$ m and 100  $\mu$ m. (C) Schematic drawing of Cytochrome P450 Family 17 Subfamily A Member 1 (CYP17A1) expression in SNpc and VTA and potential binding of local androgens on AR expressed by dopaminergic neurons. Representative example of CYP17A1 (green), NeuN (red) and GFAP (cyan) immunoreactivities in the SNpc and VTA of ENZ-, AAP- and Vehicle-treated mice. Scale bar: 250  $\mu$ m. (D) Whisker boxes represent the number of TH+ cells and AR+ cells in VTA (left panel) and in SNpc (right panel) of ENZ- and AAP- treated mice compared with respective vehicles. Statistical quantification was performed by using Mann–Whitney test. Data are represented as box and whiskers and mean  $\pm$  SEM ( $n = 4$  mice), \*  $p < 0.05$ . AAP, abiraterone acetate-prednisone; AR, androgen receptor; BBB, brain blood barrier; CYP17A1, cytochrome P450 family 17 subfamily A member 17; DA, dopamine; ENZ, enzalutamide; EPM, elevated plus maze; FST, forced swim test; GFAP, Glial Fibrillary Acidic Protein; LDB, light-dark box; NeuN, Neuronal Nuclei Antigen; OFT, open-field test; SNpc, substantia nigra pars compacta; TH, Tyrosine hydroxylase; TST, tail suspension test; vHp, ventral hippocampus; VTA, ventral tegmental area.

### 3.4. ENZ Treatment and Not AAP Specifically Altered Spatial Learning Efficiency and Cognitive Score

The role of androgen deprivation and direct AR antagonism on hippocampal functions and spatial working memory [55], spatial learning and memory, retrieval and behavioral flexibility was assessed by MWM Test (Figure 6A,B). No modification was detected in short-term and long-term memory using the probe and the retrieval tests respectively (Figure 6C, Table S3). During the flexibility phase, no change was detected in ENZ- and AAP-treated groups when compared with vehicles in terms of duration (Figure 6C) and distance crossed (Table S3). During the learning phase, distance crossed, mean speed and duration were evaluated. Neither ENZ- nor AAP-treated mice exhibited significant changes in learning abilities compared with Veh (Figure 6B, Table S3). Efficient navigation by using visual cues at disposal depends on the capacity of integration of egocentric route-based knowledge into an allocentric representation [56]. We adapted a Python Neural Network to allow the analysis of different swim strategies in six different classes (Figure 6D, Supplementary Materials Figure S5). In Veh-ENZ and Veh-AAP groups, mice used a high proportion of random swim-like scanning on D1 followed by a more efficient strategy on D3-4 as direct or rotating (Figure 6E). In ENZ compared with Vehicle mice, less successful search strategies like thigmotaxis were observed (12.5% of all strategies) contributing to a diminished cognitive score [43] only at D1 (Figure 6E) while AAP mice showed only a long time to switch towards efficient strategies (Figure S5).

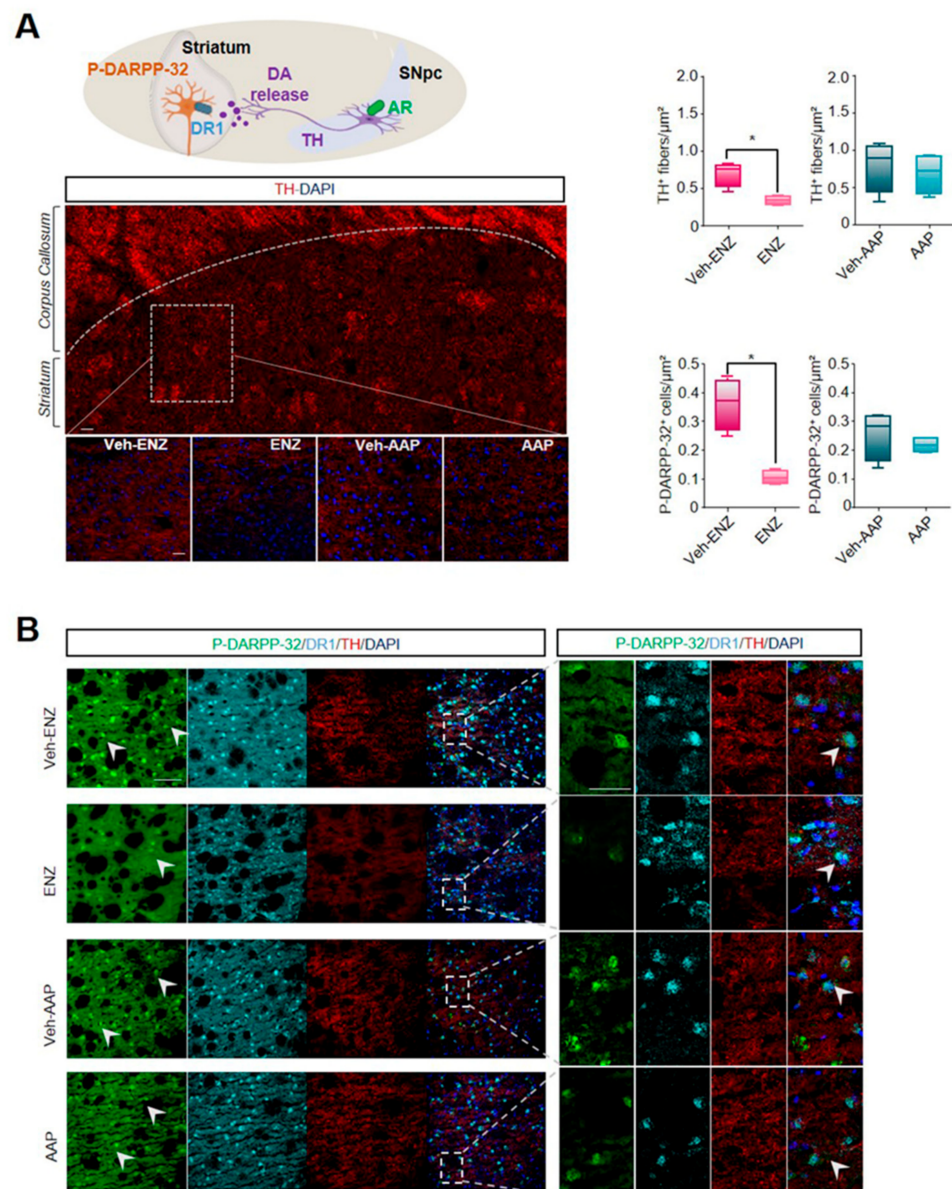


**Figure 4.** ENZ modulates midbrain dopaminergic release to striatum. Note. **(A)** Schematic representation of SNpc dopaminergic projections to striatum and consequent striatal neuronal activation. Immunofluorescence of TH<sup>+</sup>-DA striatal projections of ENZ-, AAP- and vehicle-treated mice (seen on magnification of squared areas). Scale bar: 100 μm. On the right, Whisker boxes represent TH<sup>+</sup> fibers intensity and the number of P-DARPP-32<sup>+</sup> cells in the striatum of ENZ- and AAP-treated mice compared with respective vehicles. Statistical quantifications were performed using Mann-Whitney test. Data are represented as box and whiskers of mean ± SEM (n = 4 mice), \* p < 0.05. Scale bar: 100 μm. **(B)** Representative images of Dopamine cAMP-Regulated Neuronal Phosphoprotein P-DARPP-32<sup>+</sup>—(green), DA receptor 1<sup>+</sup>—(DR1, cyan), TH<sup>+</sup>—(red) positive fibers and DAPI (blue) immunoreactivities in striatum of ENZ-, AAP- and Vehicle-treated mice. Scale bar: 25 μm and 100 μm. AAP, abiraterone acetate-prednisone; DA, dopamine; DAPI, 4',6-diamidino-2-phenylindol; ENZ, enzalutamide; P-DARPP-32, Phosphorylated form of Dopamine cAMP-Regulated Neuronal Phosphoprotein; DR1, DA receptor 1; SNpc, substantia nigra pars compacta; TH, Tyrosine hydroxylase; vHp, ventral hippocampus.

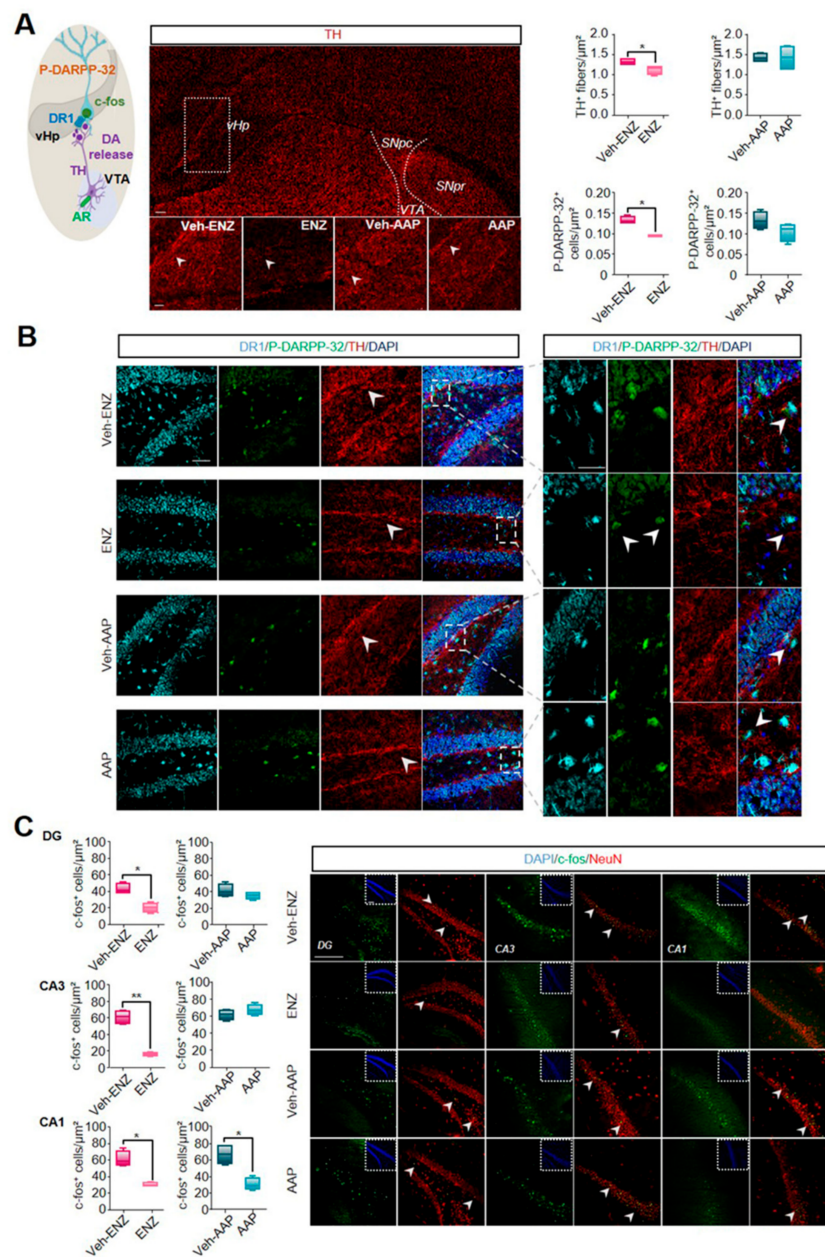


**Figure 5.** ENZ modulates midbrain dopaminergic release to ventral hippocampus. Note. (A) Schematic of dopaminergic projections to ventral hippocampus (vHp) from VTA and consequent neuronal activation. Immunofluorescence of TH<sup>+</sup>-DA projections likely arising from VTA and projecting to vHp of ENZ-, AAP- and vehicle-treated mice (seen on magnification of squared areas). Scale bar: 100  $\mu$ m. On the right, Whisker boxes represent the intensity of TH<sup>+</sup> fibers and number of P-DARPP-32<sup>+</sup> cells in the vHp (right panel) of ENZ- and AAP-treated mice compared with respective vehicles. Statistical quantifications were performed using Mann–Whitney test. Data are represented as box and whiskers of mean  $\pm$  SEM ( $n = 4$  mice), \*  $p < 0.05$ . Scale bar: 100  $\mu$ m. (B) Representative images of P-DARPP-32<sup>+</sup>—(green), DR1<sup>+</sup>—(cyan), TH<sup>+</sup>—(red) positive fibers and DAPI (blue) immunoreactivities in vHp of ENZ-, AAP- and Vehicle-treated mice. Scale bar: 25  $\mu$ m and 100  $\mu$ m. (C) Representative example of the immediate early gene (c-fos, green) and NeuN (red) immunoreactivities in the DG, CA3 and CA1 regions of vHp of ENZ-, AAP- and vehicle-treated mice. The boxed areas show DAPI (blue) immunoreactivity. On the left, whisker boxes represent the number of c-fos<sup>+</sup> cells in DG, CA3 and CA1 hippocampal areas of ENZ- and AAP-treated mice compared with respective vehicles. Statistical quantifications were performed using Mann–Whitney test. Data are represented as box and whiskers and mean  $\pm$  SEM ( $n = 4$  mice), \*  $p < 0.05$ , \*\*  $p \leq 0.01$ .

Scale bar: 100  $\mu$ m. AAP, abiraterone acetate-prednisone; CA1, cornus ammonis 1; CA3, cornus ammonis 3; c-fos, cellular oncogene c-fos; DA, dopamine; DAPI, 4',6-diamidino-2-phenylindol; DG, dentate gyrus; ENZ, enzalutamide; NeuN, Neuronal Nuclei Antigen; P-DARPP-32, Phosphorylated form of Dopamine cAMP-Regulated Neuronal Phosphoprotein; DR1, DA receptor 1; TH, Tyrosine hydroxylase; vHp, ventral hippocampus; VTA, ventral tegmental area.

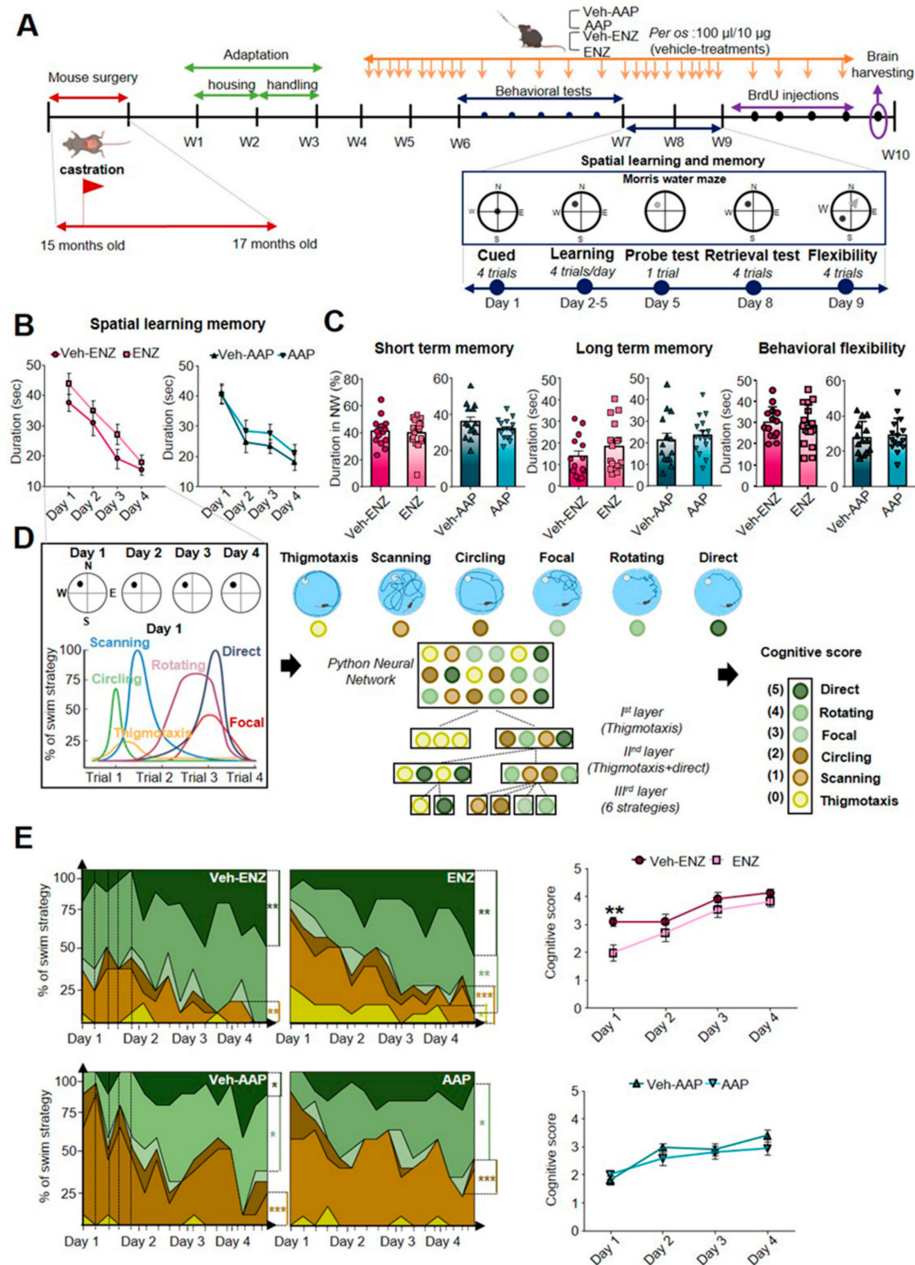


**Figure 6.** ENZ and not AAP specifically alters spatial learning efficiency and cognitive score. Note. (A) In vivo experimental time course of treatment delivery and learning and memory cognitive evaluation by Morris water maze test (MWM). MWM was performed for 7 days starting from W7 (blue arrow) with familiarization (cued) on D1, the learning phase from D2 to D5, the probe test two hours after learning trials on D5, the retrieval test on D8 and the flexibility analyzed on D9 during treatments as indicated (orange arrows). Then for 4 days mice received one BrdU injection per day (50 mg/kg) before sacrifice, brain were harvested for immunohistochemical analyses (purple arrow) and plasma were sampled. (B) Cognitive consequences of ENZ or AAP treatment compared with a vehicle on spatial learning. Bar scatter plots showing the time to reach the platform (escape latency)



during the learning phase. Statistical comparison of treatment groups was performed between vehicles ( $n = 14$ ) and treated ( $n = 16$ ) mice by repeated measures one-way ANOVA followed by Sidak's multiple comparisons test. Bars are mean  $\pm$  SEM while symbols individual data points. (C) Bar graph quantification of short-term memory (duration crossed in the target NW quadrant), long-term memory (escape latency) and behavioral flexibility (escape latency). Statistical analysis was performed between vehicle ( $n = 14$ ) and treated ( $n = 16$ ) mice data using unpaired  $t$ -test and Mann–Whitney test. (D) Left panel, schematic representation of platform positioning shown for each day of the learning phase (left panel): four trials with four different start locations (N, S, W, E) were assessed each day. An illustration of swim strategy distribution along the four trials of day 1 of learning was drawn (left). Middle panel, visual representations of swim tracks: thigmotaxis (yellow), scanning (light brown), circling (dark brown), focal (light green), rotating (middle green) and direct (dark green). Below, simplified illustration of convolution layers of the neural network used to classify swim strategies: the starting dataset of image files corresponding to tracking trajectories in all trials along the four consecutive learning days for each mouse was run throughout the first convolution layer, which distinguishes thigmotaxis from other trajectories. The second convolution layer separates thigmotaxis and direct swim from other trajectories and the third one classifies the six specific trajectories. Right panel, each training trial was scored such that more efficient strategies received higher scores according to the following scale: thigmotaxis = 0, scanning = 1, circling = 2, focal = 3, rotating = 4, direct = 5. (E) Left panel, Distribution of search swim strategies during each trial for the 4 days of learning. Swim path to target is presented as stacked area plots and percentage, vehicle ( $n = 14$ ) and treated ( $n = 16$ ). The statistical comparison of strategy evolution from D1 to D4 was assessed by chi-square test with Yates' continuity correction. Right panel, statistical analysis of cognitive scores during the 4 days of learning (4 trials/day) between vehicles ( $n = 14$ ) and treated ( $n = 16$ ) mice by repeated measures (RM) one-way ANOVA, using the Tukey's test for multiple comparisons. Data are expressed as aligned dot plots and mean  $\pm$  SEM, \*  $p < 0.05$ , \*\*  $p \leq 0.01$ , \*\*\*  $p < 0.001$ . AAP, abiraterone acetate-prednisone; BrdU, Bromodeoxyuridine; D, day; ENZ, enzalutamide; MWM, Morris water maze test; W, week.

### 3.5. ENZ Decreased *c-fos*-Related Activity of NeuN<sup>+</sup>-Neurons Whereas AAP Interfered with the Neurogenic Process in the Dorsal Hippocampus

Some neurobiological markers including *c-fos* in dHP were recognized as being involved in the neural cognitive map of space [56] and in responsiveness to learning tasks in rodents [57]. We observed that neither ENZ nor AAP significantly modified TH-staining in afferent fibers in dHP (Figure 7A). CYP17A1 immunostaining found in DG (Figure 7B), CA3 and CA1 (Figure S6), more specifically in NeuN<sup>+</sup>, supports neurosteroidogenesis and potential local production of T or DHT in dHP (Figure 7C). The co-localization of AR as potential binding sites for locally produced androgens with BrdU<sup>+</sup>-neural proliferating progenitors, DCX<sup>+</sup>-immature hippocampal neurons or NeuN<sup>+</sup>-mature neurons was thus tested (Figure 7D). We did not show AR<sup>+</sup>/BrdU<sup>+</sup> and AR<sup>+</sup>/DCX<sup>+</sup> co-expressing cells, but observed a main proportion of AR<sup>+</sup>/NeuN<sup>+</sup>-cells in dorsal DG of dHP of ENZ-, AAP- and vehicles groups (Figure 7D). The neurogenic process and BDNF expression in dHP of ENZ-treated aged mice were not altered, but enhanced BrdU<sup>+</sup>- and reduced BDNF<sup>+</sup>-cells were measured in dHP of AAP compared with Veh-AAP mice, with no consequences on mature neurons (Figure S7B). However, exploration and overtrained responding and motor activity during spatial learning have been related to CA1 neuron activity in dHP [58]. We found a significant decrease in *c-fos* expression in ENZ-treated mice in DG and CA1 in NeuN<sup>+</sup>-neurons and not in GFAP<sup>+</sup>-glial cells when compared with veh-ENZ (Figure 8). No difference was detected for *c-fos* expression in neither regions of dHP from AAP compared with Veh-AAP brain slices (Figure 8). Together, ENZ treatment is specifically associated with a decreased *c-fos*-related activity of DG and CA1 neurons in the dHP, that would sustain a deficit in exploratory performances.

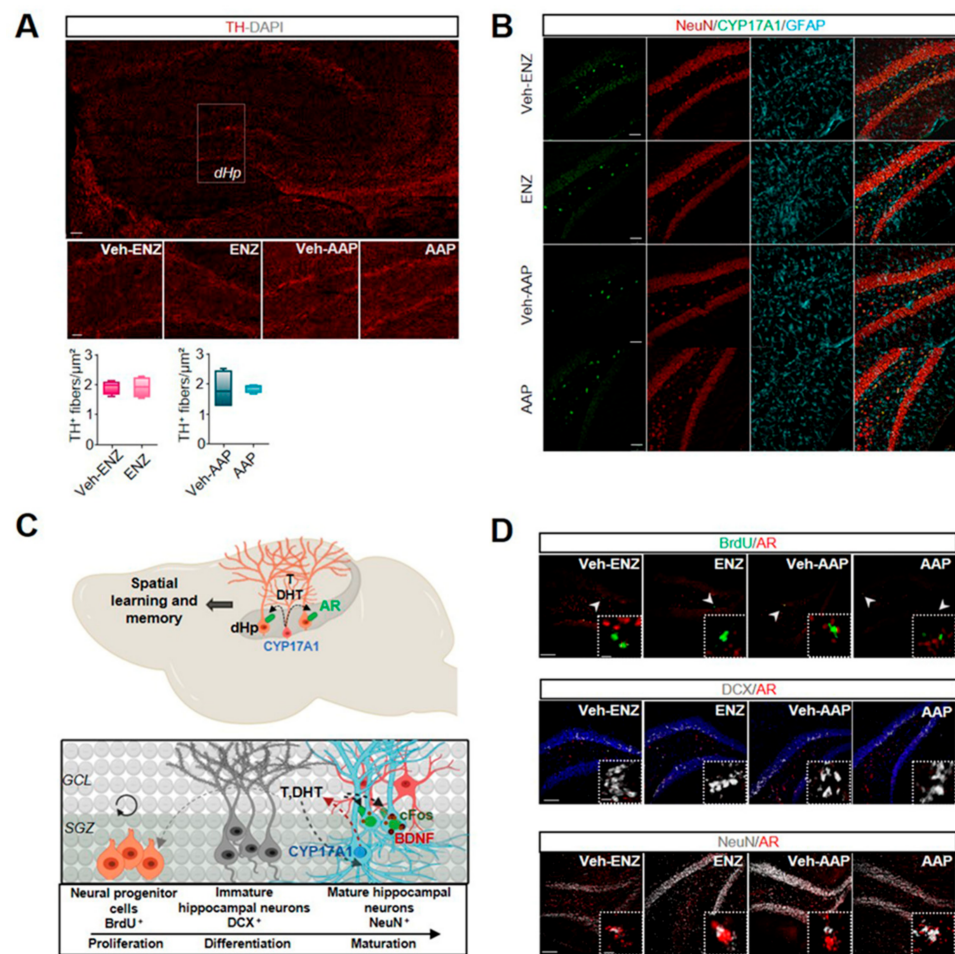


**Figure 7.** AAP and ENZ treatment impairs adult neurogenesis and neuronal activity in dorsal hippocampus respectively. Note. **(A)** Immunofluorescence of TH+–DA projections to dHP of ENZ-, AAP- and vehicle-treated mice (seen on magnification of squared areas). Whisker boxes represent the number of TH+ fibers in dHP. Statistical quantifications were performed using Mann–Whitney test. Bars are mean ± SEM (*n* = 4 mice). Scale bars: 100 μm. **(B)** Representative immunofluorescence of CYP17A1 (green), NeuN (red) and GFAP (cyan) in the DG of dHP of ENZ-, AAP- and vehicles-treated mice showing specific localization of CYP17A1 in neuronal and not glial cells. **(C)** Upper panel, schematic of mouse dorsal hippocampal (dHP) CYP17A1-mediated production of testosterone and DHT, potentially responsible for spatial learning deficits. Lower panel, hypothetical illustration of the impact of testosterone and DHT or prednisolone on neurogenesis. CYP17A1 expression by mature hippocampal neurons (neuron in light blue; astrocyte in red) of granule cell layer (GCL) of DG; AR is not expressed in neural progenitor cells stained by an anti-BrdU (orange) in the SGZ and by immature hippocampal neurons classically revealed by staining of an anti-DCX (grey) in the DG of vHP. AR expressed by mature hippocampal neurons revealed by anti-NeuN (light blue). AR (green) activation by T or DHT would control mature neuron (blue) activity as illustrated by c-fos immunolabeling. **(D)** Upper panel, representative immunolabeling of BrdU (green) and AR (red) immunofluorescence in dHP of ENZ-, AAP- and vehicles-treated mice. The boxed areas showed a magnification of lack of BrdU+/AR+ co-stained progenitor cells. Middle panel, immunolabeling of DCX (grey) and AR (red) immunofluorescence in dHP of ENZ-, AAP- and vehicle-treated mice. The boxed areas showed a magnification of lack of DCX+/AR+ co-stained immature migratory neurons in the SGZ. Lower panel, immunolabeling of NeuN (grey) and AR (red) in dHP of ENZ-, AAP- and vehicle-treated mice. The boxed areas showed a magnification of NeuN/AR co-expression in mature neurons. Scale bar: 100 μm and 50 μm. AAP, abiraterone acetate-prednisone; AR, androgen receptor; BrdU, Bromodeoxyuridine; c-fos, cellular oncogene c-fos; CYP17A1, Cytochrome P450 Family 17 Subfamily A

Member 1; DA, dopamine; DCX, doublecortin; DG, dentate gyrus; dHP, dorsal hippocampus; DHT, dihydrotestosterone; ENZ, enzalutamide; GCL, granule cell layer; GFAP, Glial Fibrillary Acidic Protein; NeuN, Neuronal Nuclei Antigen; SGZ, sub-granular zone; T, testosterone; TH, Tyrosine hydroxylase; vHP, ventral hippocampus.

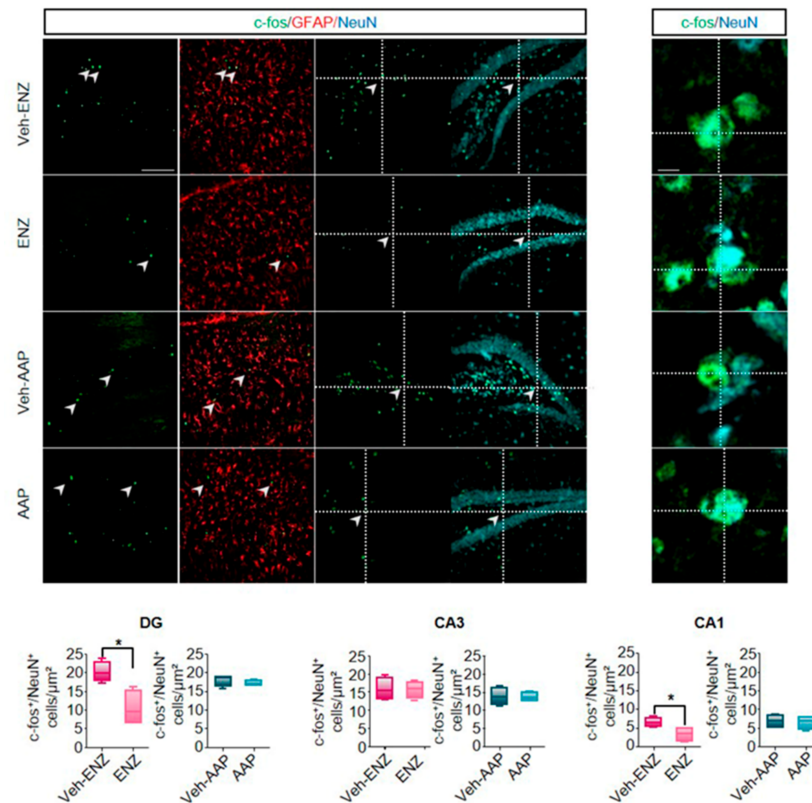


**Figure 8.** ENZ treatment impairs neuronal activity in dorsal hippocampus. Note. Representative immunolabeling and quantification of c-fos (green) expression in NeuN+—(red) or GFAP+—(cyan) cells. Intersecting lines evidenced co-localization of NeuN+—cells expressing c-fos. Whisker box plots quantification of the number of c-fos+/NeuN+—cells in the DG, CA3 and CA1 areas of dHP of ENZ- and AAP-treated mice compared with respective vehicles. Statistical quantifications were performed using Mann–Whitney test. Bars are mean  $\pm$  SEM ( $n = 4$  mice), \*  $p < 0.05$ . Scale bars: 100  $\mu$ m. AAP, abiraterone acetate-prednisone; CA1, cornus ammonis 1; CA3, cornus ammonis 3; c-fos, cellular oncogene c-fos; DG, dentate gyrus; ENZ, enzalutamide; GFAP, Glial Fibrillary Acidic Protein; NeuN, Neuronal Nuclei Antigen.

#### 4. Discussion

Clinical approaches to understanding cognitive decline in elderly patients treated for cancer are complex and the underlying neurobiological mechanisms are far from being explained. In elderly patients with mCRPC, ENZ directly targeting AR signaling or AAP (supplemented with prednisone) inhibiting CYP17A1 significantly improved OS and QoL in two clinical trials [13,59]. However, it was shown that after 12 weeks of treatment, functional assessment of cancer therapy-prostate score improved with AAP and not with ENZ and a physical well-being subscale worsened with ENZ [24]. Activation of AR signaling pathways through the local synthesis of T or DHT may regulate neurotransmission, neurogenesis and brain plasticity [60], and selective behavioral responses. Here, the first main evidence is that ENZ impacts locomotor and explorative behavior, and strength capacity likely by preventing binding of central synthesized androgens to ARs expressed by DA neurons of the SNpc and the VTA. This impairs dopaminergic release in the striatum (nigrostriatal pathway) and the vHP (mesolimbocortical pathway), leading to reduced target neurons activation. The second main fact is that ENZ reduces the cognitive score

indicative of learning efficiency deficit, here associated with less *c-fos* activation in DG and CA1 neurons of the dHP.

ADT by castration and CYP17A1 inhibition should lead to inhibition of T production and corticosterone in animals. Indeed, continuous inhibition of CYP17A1 with oral AAP in CRPC patients is safe and significantly suppresses serum androgens, estrogens and cortisol synthesis [61,62], prednisone complementation yielding physiologic cortisol levels [63]. However, low levels of T can be associated with inflammatory status in a healthy elderly population [44,45] or hypogonadism [46] while prednisone may contribute to subtle effects on immune functions [62]. Inflammatory cytokines can mediate behavioral and cognitive disturbances in both human and animal subjects [44,45], but here plasma levels of a panel of pro-inflammatory, pluripotent, anti-inflammatory, leukocyte growth and chemokine cytokines were not modified in ENZ or AAP groups compared with vehicles or control mice. By discarding the possible impact of cytokines on cognitive functions [64], we thus addressed direct central mechanisms of ENZ and AAP, both penetrating the blood–brain barrier in mice [65], potentially accounting for a large part of more fatigue and reduced activity, QoL and cognitive deficits in treated cancer elderly patients.

In aged castrated mice ENZ, and not AAP, reduced spontaneous activity and exploration, and motivation to struggle as assessed by decreased locomotor and vertical activities in OFT increased immobility in OFT arena and TST with no difference in time immobile or latency before first immobility in FST. Immobility in TST may assess the strength and energy of the movement of mice, a sign of reluctance to maintain effort [66,67], while as previously reported, activity in OFT can reflect neurotransmitter system effects on stimulus salience and behavioral activity [68,69], suggesting a key role of ENZ on motivation to explore. Interestingly, pharmacological inhibition of T conversion to DHT in non-castrated adolescent rats affected exploratory and motor behaviors in OFT by down-regulating dopaminergic activity in SNpc and VTA [70]. These behavioral observations were strengthened by the expression of androgen components [50] within the nigrostriatal circuitry in TH+ structures. We show the presence of a subset of DA neurons expressing AR but also CYP17A1 in SNpc and VTA midbrain nuclei mature neurons, providing neuroanatomical bases for the local stimulation of AR by T and/or DHT throughout the nigrostriatal and mesolimbocortical pathways. There are currently few arguments in favor of a central, midbrain, expression of CYP17A1. One is that susceptibility to develop motor dysfunctions has been linked to abnormal P450 enzyme activity [71]. Thus, CYP17A1 in both SNpc and VTA mature neurons may contribute to androgen synthesis and AR activation by midbrain DA neurons. This last assumption is here confirmed by the decrease of TH+ neuronal components expressing AR in the SNpc after ENZ treatment. This means that dopaminergic projections from SNpc to the striatum, involved in activity or action sequence initiation and performance [72], are controlled by ENZ (Figure 9). Previous studies established that activation of DR1 and DR2-expressing neurons in the striatum relays a selective control over locomotion [73] and that P-DARPP32 can be a marker of striatal MSNs dopaminergic activation [74]. Accordingly, a diminished P-DARPP32 in striatal neurons expressing at least D1R of ENZ mice suggests that AR antagonism can lead to inhibition of striatal DA release and activity, and of motor and/or exploratory behavior. Despite the expression of CYP17A1 in SNpc and VTA, no effect of AAP is observed, potentially attributed to the weak passage across the BBB and/or a possible steroidal conversion of AA with inefficient blockage of steroidogenesis [62]. In contrast, some seizure and psycho-motor troubles [20], as well as mental impairments [75], have already been described in clinical studies with ENZ. ENZ which is able to cross the BBB [76,77] can reduce the activity of the AR likely expressed in some brain areas, but also was suspected to exert off-target binding to, and inhibition of, the GABA<sub>A</sub> receptor/channel as previously described [78], all suggesting that the impact of ENZ compared with AAP on mouse behavior and neurobiological substrates may be affected by the specific degree of BBB penetration.

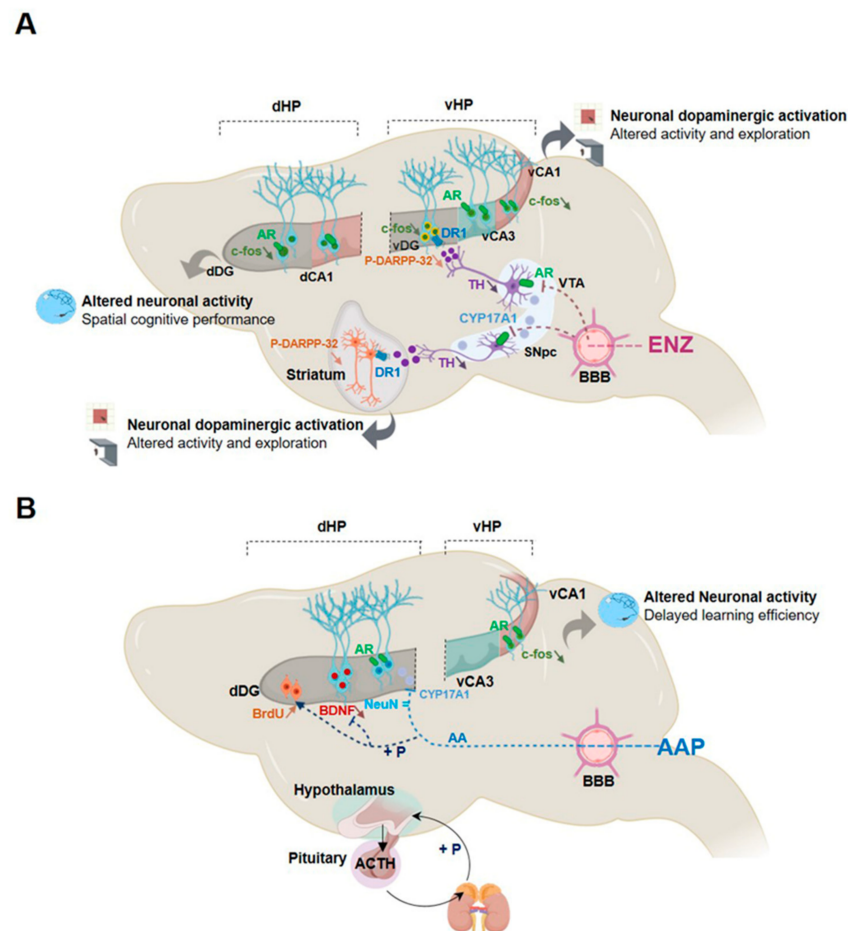


**Figure 9.** Schematic illustration of the central action of novel generation hormone therapy targeting the androgen signaling axis, abiraterone acetate+prednisone (AAP) and enzalutamide (ENZ) in aged castrated mice. Note. **(A)** ENZ which is able to cross the blood–brain barrier (BBB) can bind and inhibit ARs expressed in peripheral and brain organs. More specifically, CYP17A1 and AR are localized in both SNpc and VTA neurons in aged castrated mouse brains. ENZ leads to reduced P-DARPP-32 activated signaling in mature neurons expressing DR1 in the striatum through the nigrostriatal pathway and in the vHP via part of the mesolimbocortical pathway. This inhibition of DA-expressing afferents likely accounts for diminished locomotor activity and exploration behavior. ENZ also depressed mature neuron activity evidenced by c-fos expression in dHP potentially responsible for an altered spatial cognitive performance. **(B)** AAP is a prodrug, generating abiraterone selective for CYP17A1 enzyme activity, thus inhibiting androgen biosynthesis in the testis and the adrenal gland, but potentially in the VTA and SNpc. AA may have the ability to cross the BBB. In order to avoid cortisol deficiency, the treatment is combined with chronic use of prednisone (P) sufficient to activate the HPA-related feedback loop and to reduce the plasma ACTH level allowing physiological cortisol production in patients. CYP17A1 and AR are expressed in the dHP, and here the AAP effect on proliferation of precursor cells and inhibition of BDNF production without modification of mature neurons would hypothetically involve glucocorticoids receptors. In the vHP, the AAP-evoked reduction of c-Fos in mature neurons can sustain the delay in efficiency in spatial learning acquisition. AA, abiraterone acetate; AAP, abiraterone acetate-prednisone; ACTH, adrenocorticotrophic hormone; AR, androgen receptor; BBB, blood–brain barrier; BDNF, Brain-derived neurotrophic factor; c-fos, cellular oncogene c-fos; CYP17A1, Cytochrome P450 Family 17 Subfamily A Member 1; DA, dopamine; dHP, dorsal hippocampus; ENZ, enzalutamide; HPA, hypothalamic–pituitary–adrenal; P, prednisone; P-DARPP-32, Phosphorylated form of Dopamine cAMP-Regulated Neuronal Phosphoprotein; DR1, DA receptor 1; SNpc, substantia nigra pars compacta; vHP, ventral hippocampus; VTA, ventral tegmental area.

DA transmission from VTA to the hippocampus has been associated with novelty detection and motivation to explore [48,49], suggesting that the observed ENZ-induced less motivation to explore, also involved the mesolimbocortical pathway. Fewer TH<sup>+</sup>-neurons expressing AR in the VTA and TH<sup>+</sup>—positive fibers in the vHp of ENZ mice indicate mesolimbocortical circuit involvement. This was evidenced by reduced DARPP32 phosphorylation and c-fos expression through the DG, CA1 and CA3, as key markers of DA neuron activity [79]. In addition, AR is also found throughout the vHp supporting sensitivity of DG, CA3, and mostly CA1 to local steroidogenesis [80]. As in the study showing that reduced neuronal activity in the vHP constitutes a neurobiological substrate of reduced exploratory behaviors [53], the ENZ-evoked inhibition of vHP neuron activity should contribute to depressing motivation to explore and/or to effort of aged castrated mice.

The central role of androgens in spatial learning and memory abilities has been described [81–83] but in the MWM test, no macroscopic impairment was detected in learning abilities, short- and long-term memories and behavioral flexibility. However, a detailed classification of swimming paths by dividing them into different “exploration strategies” [40], yielding a score based on animal relevance to spatial learning [43], highlighted that ENZ exhibit a lower cognitive score than Veh-ENZ mice. It results in the prolonged occurrence of ineffective thigmotaxis behavior search strategy resulting in reduced efficacy in spatial exploration. AAP did impact cognitive score when compared with veh-AAP, showing only a slower acquisition of more effective strategies.

The hippocampus is considered “the neural substrate of a cognitive map of space” [57]. dHP in particular is required for the normal acquisition of a spatial memory task and learning [84], and hippocampal adult neurogenesis is necessary for proper hippocampus-dependent spatial learning [85,86]. Stimulating effects of T or DHT on SVZ progenitor proliferation [87–89] and on newborn neuron survival [90], can be related to CYP17A1 expression in rodent hippocampus [91], mainly in CA1-CA3 pyramidal neurons [92]. In our aged castrated mouse model, CYP17A1 appears sparsely but specifically expressed in mature dHP neurons. In dHP, we also found AR expressed rather on dHP mature neurons instead of neural proliferating cells or immature hippocampal neurons, likely insensible to androgens. Accordingly, neither ENZ nor AAP modifies vHp neurogenesis and the number of mature neurons was similarly unmodified in dHP after treatments. Even if one observes that AAP treatment increased the number of proliferating neural cells and decreased hippocampal expression of BDNF, the lack of AR expression in these cells suggests the contribution of the exogenously co-administered prednisone. Consistently, the hippocampus highly expresses glucocorticoid receptors [93], and exposure to a low concentration of glucocorticoid enhances the proliferation of progenitor cells and suppresses differentiation into neurons, through decreased BDNF [93,94]. AAP-induced reduction in BDNF expression may support the slower improvement of ongoing swimming strategies in MWM, BDNF facilitating the short-term plasticity necessary for rapid switches in swim paths [95]. Importantly, to understand how ENZ reduces performances in learning strategies during the MWM, we tested VTA as the presumed source of DA within the dHP [96], and discard VTA input influence. However, c-fos expression is a mediator of dopaminergic activity in a number of cortical regions [97] and its inhibition in dCA3 has been shown to slow down the process. Interestingly, ENZ leads to a marked inhibition of c-fos expression, indicating that antagonizing androgen signaling in dHP can be associated with alteration of efficient scanning of the environment to achieve the goal.

## 5. Conclusions

Currently, the vast panel of therapeutic tools and options, adapted to one type and subtypes of cancers, offers major prospects in terms of improving OS, but also addresses the issue of maintaining the best QoL for cancer patients. This challenge is accompanied by the difficulty for cancer patients with coping, the role of co-morbidities and aging. In elderly men with mCRPC, it was found that NGHTs such as ENZ or AAP significantly improved OS and QoL benefits compared with chemotherapy. With the goal of better management

of mCRPC patients, it becomes critical to understand the role of ENZ and AAP on the incidence, severity of cognitive impairments and impact on QoL in mCRPC patients. Our original and key findings in a preclinical model of castrated aged mice is that ENZ alters activity and exploration, as well as cognitive performances, likely suggesting treatment impact of neurofatigue and cognitive functions in elderly patients. Our results show the importance of robustly exploring hormone treatment side effects, including fatigue and cognition that would impact QoL, autonomy and adherence, to evaluate suboptimal clinical responses in this population at cognitive risk.

**Supplementary Materials:** The following are available online at <https://www.mdpi.com/article/10.3390/cancers13143518/s1>, Figure S1: ENZ or AAP have no impact on body weight gain. Figure S2: ENZ but not AAP decreases dopaminergic activation of striatal medium spiny neurons. Figure S3: Androgen receptors are expressed by mature neurons of ventral hippocampus. Figure S4: ENZ but not AAP decreases dopaminergic activation of mature neurons of ventral hippocampus. Figure S5: ENZ or AAP treatment impacts on learning strategy trend overtime. Figure S6: CYP17A1 expression in CA3 and CA1 of dorsal hippocampus. Figure S7: AAP treatment alters neurogenesis with no major effect on mature neurons. Table S1: Lack of effect of ENZ or AAP on plasma pro-inflammatory, pluripotent, anti-inflammatory, leukocyte growth and chemotactic cytokines. Table S2: Summary of the behavioral phenotypes of non-treated non-castrated aged mice. Table S3: Summary of the behavioral phenotypes of aged castrated mice treated with ENZ or AAP.

**Author Contributions:** Conceptualization, H.C., M.L., F.J.; methodology, M.D., C.C., C.N., L.D., L.G.; software, C.N., D.S., T.A.S.; validation, M.D., H.C.; formal analysis, C.N., M.D., T.A.S.; investigation, C.N., M.D., H.C.; data curation, C.N., M.D., L.D.; writing—original draft preparation, H.C., C.N.; writing—review and editing, H.C.; supervision, H.C.; project administration, H.C.; funding acquisition, H.C., F.J. All authors have read and agreed to the published version of the manuscript.

**Funding:** This study was independently funded by Janssen Pharmaceutica N.V. This work was also supported by The ligue nationale contre le cancer (Plate-forme Cancer and cognition), Région Normandie RIN and les Fonds Européens du Développement Régional (FEDER) CancerCOG, Normandy Rouen University and Inserm.

**Institutional Review Board Statement:** The study did not involve humans. The number and the suffering of animals were minimized in accordance with the guidelines of the European Parliament and Council Directive (2010/63/EU) 3/EU) and ARRIVE (Animal Research: Reporting of In Vivo Experiments) 2.0 guidelines. This project was approved by the “Comité d’Ethique Normandie en Matière d’Expérimentation Animale” and the French Research Minister (#7866-2016112115226170 v5) and carried out under the supervision of authorized operators (HC and MD).

**Data Availability Statement:** Data supporting reported results are available upon request.

**Acknowledgments:** This study was enabled by the possible free accessibility to the deep learning framework Chainer. We are grateful to Lorenzo Genuardi for help in the modification of the python program and systematic evaluation of the classification accuracy of learning strategies in Morris water maze test. We thank the PRIMACEN platform (Normandy Rouen University, France) for imaging equipment and Arnaud Arabo and Julie Maucotel, for animal housing and care and for access to the behavioral equipments of the Biological Resources Department (Normandie Rouen University, France).

**Conflicts of Interest:** Celeste Nicola, Martine Dubois, Cynthia Campart, Tareq Al Sagheer, Laurence Desrues, Damien Schapman, Ludovic Galas and Marie Lange have no biomedical financial interests or no conflicts of interest to declare. Florence Joly reports having received lecture and consulting fees for from Janssen-Cilag, Astellas Pharma, Bayer, Sanofi and a research funding from Astellas Pharma. Hélène Castel reports having received a research funding from Janssen-Cilag.

## References

1. Deprez, S.; Kesler, S.R.; Saykin, A.J.; Silverman, D.H.S.; de Ruiter, M.B.; McDonald, B.C. International Cognition and Cancer Task Force Recommendations for Neuroimaging Methods in the Study of Cognitive Impairment in Non-CNS Cancer Patients. *J. Natl. Cancer Inst.* **2018**, *110*, 223–231. [[CrossRef](#)]
2. Amidi, A.; Agerbæk, M.; Wu, L.M.; Pedersen, A.D.; Mehlsen, M.; Clausen, C.R.; Demontis, D.; Børglum, A.D.; Harbøll, A.; Zachariae, R. Changes in cognitive functions and cerebral grey matter and their associations with inflammatory markers, endocrine markers, and APOE genotypes in testicular cancer patients undergoing treatment. *Brain Imaging Behav.* **2017**, *11*, 769–783. [[CrossRef](#)]
3. Amidi, A.; Hosseini, S.M.H.; Leemans, A.; Kesler, S.R.; Agerbæk, M.; Wu, L.M.; Zachariae, R. Changes in Brain Structural Networks and Cognitive Functions in Testicular Cancer Patients Receiving Cisplatin-Based Chemotherapy. *J. Natl. Cancer Inst.* **2017**, *109*. [[CrossRef](#)] [[PubMed](#)]
4. Lange, M.; Joly, F.; Vardy, J.; Ahles, T.; Dubois, M.; Tron, L.; Winocur, G.; De Ruiter, M.B.; Castel, H. Cancer-related cognitive impairment: An update on state of the art, detection, and management strategies in cancer survivors. *Ann. Oncol. Off. J. Eur. Soc. Med. Oncol.* **2019**, *30*, 1925–1940. [[CrossRef](#)] [[PubMed](#)]
5. Winocur, G.; Johnston, I.; Castel, H. Chemotherapy and cognition: International cognition and cancer task force recommendations for harmonising preclinical research. *Cancer Treat. Rev.* **2018**, *69*, 72–83. [[CrossRef](#)] [[PubMed](#)]
6. Joly, F.; Heutte, N.; Duclos, B.; Noal, S.; Léger-Hardy, I.; Dauchy, S.; Longato, N.; Desrues, L.; Houede, N.; Lange, M.; et al. Prospective Evaluation of the Impact of Antiangiogenic Treatment on Cognitive Functions in Metastatic Renal Cancer. *Eur. Urol. Focus* **2016**, *2*, 642–649. [[CrossRef](#)]
7. Joly, F.; Castel, H.; Tron, L.; Lange, M.; Vardy, J. Potential Effect of Immunotherapy Agents on Cognitive Function in Cancer Patients. *J. Natl. Cancer Inst.* **2020**, *112*, 123–127. [[CrossRef](#)]
8. Cherrier, M.M.; Higano, C.S. Impact of androgen deprivation therapy on mood, cognition, and risk for AD. *Urol. Oncol.* **2020**, *38*, 53–61. [[CrossRef](#)]
9. McGinnis, G.J.; Friedman, D.; Young, K.H.; Torres, E.R.; Thomas, C.R., Jr.; Gough, M.J.; Raber, J. Neuroinflammatory and cognitive consequences of combined radiation and immunotherapy in a novel preclinical model. *Oncotarget* **2017**, *8*, 9155–9173. [[CrossRef](#)]
10. Siegel, R.L.; Miller, K.D.; Jemal, A. Cancer statistics, 2018. *CA A Cancer J. Clin.* **2018**, *68*, 7–30. [[CrossRef](#)]
11. Steliarova-Foucher, E.; O’Callaghan, M.; Ferlay, J.; Masuyer, E.; Rosso, S.; Forman, D.; Bray, F.; Comber, H. The European Cancer Observatory: A new data resource. *Eur. J. Cancer* **2015**, *51*, 1131–1143. [[CrossRef](#)] [[PubMed](#)]
12. Mottet, N.; Bellmunt, J.; Bolla, M.; Briers, E.; Cumberbatch, M.G.; De Santis, M.; Fossati, N.; Gross, T.; Henry, A.M.; Joniau, S.; et al. EAU-ESTRO-SIOG Guidelines on Prostate Cancer. Part 1: Screening, Diagnosis, and Local Treatment with Curative Intent. *Eur. Urol.* **2017**, *71*, 618–629. [[CrossRef](#)] [[PubMed](#)]
13. Lorient, Y.; Bianchini, D.; Ileana, E.; Sandhu, S.; Patrikidou, A.; Pezaro, C.; Albiges, L.; Attard, G.; Fizazi, K.; De Bono, J.S.; et al. Antitumour activity of abiraterone acetate against metastatic castration-resistant prostate cancer progressing after docetaxel and enzalutamide (MDV3100). *Ann. Oncol. Off. J. Eur. Soc. Med. Oncol.* **2013**, *24*, 1807–1812. [[CrossRef](#)]
14. Armstrong, A.J. New treatment options in castration-resistant prostate cancer. *J. Natl. Compr. Cancer Netw. JNCCN* **2015**, *13*, 690–693. [[CrossRef](#)]
15. Attard, G.; Reid, A.H.; Yap, T.A.; Raynaud, F.; Dowsett, M.; Settattree, S.; Barrett, M.; Parker, C.; Martins, V.; Folkard, E.; et al. Phase I clinical trial of a selective inhibitor of CYP17, abiraterone acetate, confirms that castration-resistant prostate cancer commonly remains hormone driven. *J. Clin. Oncol. Off. J. Am. Soc. Clin. Oncol.* **2008**, *26*, 4563–4571. [[CrossRef](#)] [[PubMed](#)]
16. Wong, Y.N.; Ferraldeschi, R.; Attard, G.; de Bono, J. Evolution of androgen receptor targeted therapy for advanced prostate cancer. *Nature reviews. Clin. Oncol.* **2014**, *11*, 365–376. [[CrossRef](#)]
17. Beer, T.M.; Armstrong, A.J.; Rathkopf, D.E.; Lorient, Y.; Sternberg, C.N.; Higano, C.S.; Iversen, P.; Bhattacharya, S.; Carles, J.; Chowdhury, S.; et al. Enzalutamide in Metastatic Prostate Cancer before Chemotherapy. *N. Engl. J. Med.* **2014**, *371*, 424–433. [[CrossRef](#)]
18. De Bono, J.S.; Logothetis, C.J.; Molina, A.; Fizazi, K.; North, S.; Chu, L.; Chi, K.N.; Jones, R.J.; Goodman, O.B.; Saad, F.; et al. Abiraterone and Increased Survival in Metastatic Prostate Cancer. *N. Engl. J. Med.* **2011**, *364*, 1995–2005. [[CrossRef](#)]
19. Antonarakis, E.S. Enzalutamide: The emperor of all anti-androgens. *Transl. Androl. Urol.* **2013**, *2*, 119–120. [[CrossRef](#)]
20. Scher, H.I.; Fizazi, K.; Saad, F.; Taplin, M.-E.; Sternberg, C.N.; Miller, K.; de Wit, R.; Mulders, P.; Chi, K.N.; Shore, N.D.; et al. Increased Survival with Enzalutamide in Prostate Cancer after Chemotherapy. *N. Engl. J. Med.* **2012**, *367*, 1187–1197. [[CrossRef](#)]
21. Lange, M.; Lavie, H.; Castel, H.; Heutte, N.; Leconte, A.; Léger, I.; Giffard, B.; Capel, A.; Dubois, M.; Clarisse, B.; et al. Correction to: Impact of new generation hormone-therapy on cognitive function in elderly patients treated for a metastatic prostate cancer: Cog-Pro trial protocol. *BMC Cancer* **2018**, *18*, 110. [[CrossRef](#)]
22. Lange, M.; Rigal, O.; Clarisse, B.; Giffard, B.; Sevin, E.; Barillet, M.; Eustache, F.; Joly, F. Cognitive dysfunctions in elderly cancer patients: A new challenge for oncologists. *Cancer Treat. Rev.* **2014**, *40*, 810–817. [[CrossRef](#)]
23. Satoh, T.; Uemura, H.; Tanabe, K.; Nishiyama, T.; Terai, A.; Yokomizo, A.; Nakatani, T.; Imanaka, K.; Ozono, S.; Akaza, H. A phase 2 study of abiraterone acetate in Japanese men with metastatic castration-resistant prostate cancer who had received docetaxel-based chemotherapy. *Jpn. J. Clin. Oncol.* **2014**, *44*, 1206–1215. [[CrossRef](#)] [[PubMed](#)]



24. Khalaf, D.; Sunderland, K.; Eigl, B.J.; Finch, D.L.; Oja, C.D.; Vergidis, J.; Parimi, S.; Zulfiqar, M.; Gleave, M.; Chi, K.N. Assessment of quality of life (QOL), cognitive function and depression in a randomized phase II study of abiraterone acetate (ABI) plus prednisone (P) vs. enzalutamide (ENZA) for metastatic castrate-resistant prostate cancer (mCRPC). *J. Clin. Oncol.* **2017**, *35*, 5036. [[CrossRef](#)]
25. Shore, N.D.; Saltzstein, D.R.; Sieber, P.R.; Mehlhaff, B.; Gervasi, L.; Phillips, J.; Wong, Y.-N.; Pei, H.; McGowan, T. Real-world study of enzalutamide and abiraterone acetate (with prednisone) tolerability (REAACT): Results. *J. Clin. Oncol.* **2018**, *36*, 296. [[CrossRef](#)]
26. Thiery-Vuillemin, A.; Poulsen, M.H.; Lagneau, E.; Ploussard, G.; Birtle, A.; Dourthe, L.-M.; Beal-Ardisson, D.; Pintus, E.; Trepiakas, R.; Lefresne, F.; et al. Impact of Abiraterone Acetate plus Prednisone or Enzalutamide on Patient-reported Outcomes in Patients with Metastatic Castration-resistant Prostate Cancer: Final 12-mo Analysis from the Observational AQUARiUS Study. *Eur. Urol.* **2020**, *77*, 380–387. [[CrossRef](#)]
27. Pelletier, G. Steroidogenic Enzymes in the Brain: Morphological Aspects. In *Progress in Brain Research*; Martini, L., Ed.; Elsevier: Amsterdam, The Netherlands, 2010; Chapter 11; Volume 181, pp. 193–207.
28. Schmidt, K.L.; Pradhan, D.S.; Shah, A.H.; Charlier, T.D.; Chin, E.H.; Soma, K.K. Neurosteroids, immunosteroids, and the Balkanization of endocrinology. *Gen. Comp. Endocrinol.* **2008**, *157*, 266–274. [[CrossRef](#)] [[PubMed](#)]
29. Yamada, H.; Kominami, S.; Takemori, S.; Kitawaki, J.; Kataoka, Y. Immunohistochemical Localization of Cytochrome P450 Enzymes in the Rat Brain, Considering the Steroid-Synthesis in the Neurons. *Acta Histochem. Cytochem.* **1997**, *30*, 609–616. [[CrossRef](#)]
30. Hojo, Y.; Hattori, T.A.; Enami, T.; Furukawa, A.; Suzuki, K.; Ishii, H.T.; Mukai, H.; Morrison, J.H.; Janssen, W.G.; Kominami, S.; et al. Adult male rat hippocampus synthesizes estradiol from pregnenolone by cytochromes P45017alpha and P450 aromatase localized in neurons. *Proc. Natl. Acad. Sci. USA* **2004**, *101*, 865–870. [[CrossRef](#)]
31. Shibuya, K.; Takata, N.; Hojo, Y.; Furukawa, A.; Yasumatsu, N.; Kimoto, T.; Enami, T.; Suzuki, K.; Tanabe, N.; Ishii, H.; et al. Hippocampal cytochrome P450s synthesize brain neurosteroids which are paracrine neuromodulators of synaptic signal transduction. *Biochim. Biophys. Acta (BBA) Gen. Subj.* **2003**, *1619*, 301–316. [[CrossRef](#)]
32. Costa, G.; Serra, M.; Pintori, N.; Casu, M.A.; Zanda, M.T.; Murtas, D.; De Luca, M.A.; Simola, N.; Fattore, L. The novel psychoactive substance methoxetamine induces persistent behavioral abnormalities and neurotoxicity in rats. *Neuropharmacology* **2019**, *144*, 219–232. [[CrossRef](#)] [[PubMed](#)]
33. Prut, L.; Belzung, C. The open field as a paradigm to measure the effects of drugs on anxiety-like behaviors: A review. *Eur. J. Pharmacol.* **2003**, *463*, 3–33. [[CrossRef](#)]
34. Muller, C.P.; Cunningham, K.A. *Handbook of the Behavioral Neurobiology of Serotonin*; Academic Press: Cambridge, MA, USA, 2020.
35. Lister, R.G. The use of a plus-maze to measure anxiety in the mouse. *Psychopharmacology* **1987**, *92*, 180–185. [[CrossRef](#)] [[PubMed](#)]
36. Steru, L.; Chermat, R.; Thierry, B.; Simon, P. The tail suspension test: A new method for screening antidepressants in mice. *Psychopharmacology* **1985**, *85*, 367–370. [[CrossRef](#)]
37. Porsolt, R.D.; Bertin, A.; Jalfre, M. Behavioral despair in mice: A primary screening test for antidepressants. *Arch. Int. Pharmacodyn. Ther.* **1977**, *229*, 327–336. [[PubMed](#)]
38. Dubois, M.; Lapinte, N.; Villier, V.; Lecointre, C.; Roy, V.; Tonon, M.C.; Gandolfo, P.; Joly, F.; Hilber, P.; Castel, H. Chemotherapy-induced long-term alteration of executive functions and hippocampal cell proliferation: Role of glucose as adjuvant. *Neuropharmacology* **2014**, *79*, 234–248. [[CrossRef](#)]
39. Morris, R.G.M.; Garrud, P.; Rawlins, J.N.P.; O'Keefe, J. Place navigation impaired in rats with hippocampal lesions. *Nature* **1982**, *297*, 681–683. [[CrossRef](#)]
40. Graziano, A.; Petrosini, L.; Bartoletti, A. Automatic recognition of explorative strategies in the Morris water maze. *J. Neurosci. Methods* **2003**, *130*, 33–44. [[CrossRef](#)]
41. Higaki, A.; Mogi, M.; Iwanami, J.; Min, L.-J.; Bai, H.-Y.; Shan, B.-S.; Kan-no, H.; Ikeda, S.; Higaki, J.; Horiuchi, M. Recognition of early stage thigmotaxis in Morris water maze test with convolutional neural network. *PLoS ONE* **2018**, *13*, e0197003. [[CrossRef](#)]
42. Tokui, S.; Oono, K.; Hido, S.; Clayton, J. Chainer. A next-generation open source framework for deep learning. In Proceedings of the Workshop on Machine Learning Systems (LearningSys) in the 29th Annual Conference on Neural Information Processing Systems (NIPS), Montréal, QC, Canada, 12 December 2015; pp. 1–6.
43. Illouz, T.; Madar, R.; Louzoun, Y.; Griffioen, K.J.; Okun, E. Corrigendum to “Unraveling cognitive traits using the Morris water maze unbiased strategy classification (MUST-C) algorithm”. *Brain Behav. Immun.* **2017**, *61*, 386. [[CrossRef](#)] [[PubMed](#)]
44. Tsilidis, K.K.; Rohrmann, S.; McGlynn, K.A.; Nyante, S.J.; Lopez, D.S.; Bradwin, G.; Feinleib, M.; Joshu, C.E.; Kanarek, N.; Nelson, W.G.; et al. Association between endogenous sex steroid hormones and inflammatory biomarkers in US men. *Andrology* **2013**, *1*, 919–928. [[CrossRef](#)] [[PubMed](#)]
45. Maggio, M.; Basaria, S.; Ble, A.; Lauretani, F.; Bandinelli, S.; Ceda, G.P.; Valenti, G.; Ling, S.M.; Ferrucci, L. Correlation between testosterone and the inflammatory marker soluble interleukin-6 receptor in older men. *J. Clin. Endocrinol. Metab.* **2006**, *91*, 345–347. [[CrossRef](#)] [[PubMed](#)]
46. Bobjer, J.; Katrinaki, M.; Tsatsanis, C.; Lundberg Giwerzman, Y.; Giwerzman, A. Negative association between testosterone concentration and inflammatory markers in young men: A nested cross-sectional study. *PLoS ONE* **2013**, *8*, e61466. [[CrossRef](#)]
47. Guitart-Masip, M.; Fuentemilla, L.; Bach, D.R.; Huys, Q.J.M.; Dayan, P.; Dolan, R.J.; Duzel, E. Action Dominates Valence in Anticipatory Representations in the Human Striatum and Dopaminergic Midbrain. *J. Neurosci.* **2011**, *31*, 7867–7875. [[CrossRef](#)] [[PubMed](#)]

48. Jeewajee, A.; Lever, C.; Burton, S.; O'Keefe, J.; Burgess, N. Environmental novelty is signaled by reduction of the hippocampal theta frequency. *Hippocampus* **2008**, *18*, 340–348. [[CrossRef](#)] [[PubMed](#)]
49. Ghanbarian, E.; Motamedi, F. Ventral tegmental area inactivation suppresses the expression of CA1 long term potentiation in anesthetized rat. *PLoS ONE* **2013**, *8*, e58844. [[CrossRef](#)]
50. Kritzer, M.F. Selective colocalization of immunoreactivity for intracellular gonadal hormone receptors and tyrosine hydroxylase in the ventral tegmental area, substantia nigra, and retrorubral fields in the rat. *J. Comp. Neurol.* **1997**, *379*, 247–260. [[CrossRef](#)]
51. Simerly, R.B.; Chang, C.; Muramatsu, M.; Swanson, L.W. Distribution of androgen and estrogen receptor mRNA-containing cells in the rat brain: An in situ hybridization study. *J. Comp. Neurol.* **1990**, *294*, 76–95. [[CrossRef](#)]
52. Martig, A.K.; Mizumori, S.J. Ventral tegmental area disruption selectively affects CA1/CA2 but not CA3 place fields during a differential reward working memory task. *Hippocampus* **2011**, *21*, 172–184. [[CrossRef](#)]
53. Fanselow, M.S.; Dong, H.-W. Are the dorsal and ventral hippocampus functionally distinct structures? *Neuron* **2010**, *65*, 7–19. [[CrossRef](#)]
54. Heckman, P.R.A.; Blokland, A.; Bollen, E.P.P.; Prickaerts, J. Phosphodiesterase inhibition and modulation of corticostriatal and hippocampal circuits: Clinical overview and translational considerations. *Neurosci. Biobehav. Rev.* **2018**, *87*, 233–254. [[CrossRef](#)]
55. Meyer, K.; Korz, V. Estrogen receptor  $\alpha$  functions in the regulation of motivation and spatial cognition in young male rats. *PLoS ONE* **2013**, *8*, e79303. [[CrossRef](#)]
56. Garthe, A.; Kempermann, G. An old test for new neurons: Refining the Morris water maze to study the functional relevance of adult hippocampal neurogenesis. *Front. Neurosci.* **2013**, *7*, 63. [[CrossRef](#)]
57. Bannerman, D.M.; Rawlins, J.N.; McHugh, S.B.; Deacon, R.M.; Yee, B.K.; Bast, T.; Zhang, W.N.; Pothuizen, H.H.; Feldon, J. Regional dissociations within the hippocampus—memory and anxiety. *Neurosci. Biobehav. Rev.* **2004**, *28*, 273–283. [[CrossRef](#)] [[PubMed](#)]
58. Gall, C.M.; Hess, U.S.; Lynch, G. Mapping Brain Networks Engaged by, and Changed by, Learning. *Neurobiol. Learn. Mem.* **1998**, *70*, 14–36. [[CrossRef](#)] [[PubMed](#)]
59. Ryan, C.J.; Smith, M.R.; Fizazi, K.; Saad, F.; Mulders, P.F.; Sternberg, C.N.; Miller, K.; Logothetis, C.J.; Shore, N.D.; Small, E.J.; et al. Abiraterone acetate plus prednisone versus placebo plus prednisone in chemotherapy-naive men with metastatic castration-resistant prostate cancer (COU-AA-302): Final overall survival analysis of a randomised, double-blind, placebo-controlled phase 3 study. *Lancet Oncol.* **2015**, *16*, 152–160. [[CrossRef](#)]
60. Diotel, N.; Charlier, T.D.; Lefebvre d' Hellencourt, C.; Couret, D.; Trudeau, V.L.; Nicolau, J.C.; Meilhac, O.; Kah, O.; Pellegrini, E. Steroid transport, local synthesis, and signaling within the brain: Roles in neurogenesis, neuroprotection, and sexual behaviors. *Front. Neurosci.* **2018**, *12*, 84. [[CrossRef](#)] [[PubMed](#)]
61. Attard, G.; Merseburger, A.S.; Arlt, W.; Sternberg, C.N.; Feyereabend, S.; Berruti, A.; Joniau, S.; Géczi, L.; Lefresne, F.; Lahaye, M.; et al. Assessment of the Safety of Glucocorticoid Regimens in Combination With Abiraterone Acetate for Metastatic Castration-Resistant Prostate Cancer: A Randomized, Open-label Phase 2 Study. *JAMA Oncol.* **2019**, *5*, 1159–1167. [[CrossRef](#)] [[PubMed](#)]
62. Attard, G.; Reid, A.H.; Auchus, R.J.; Hughes, B.A.; Cassidy, A.M.; Thompson, E.; Oommen, N.B.; Folkard, E.; Dowsett, M.; Arlt, W.; et al. Clinical and biochemical consequences of CYP17A1 inhibition with abiraterone given with and without exogenous glucocorticoids in castrate men with advanced prostate cancer. *J. Clin. Endocrinol. Metab.* **2012**, *97*, 507–516. [[CrossRef](#)] [[PubMed](#)]
63. Auchus, R.J.; Yu, M.K.; Nguyen, S.; Mundle, S.D. Use of prednisone with abiraterone acetate in metastatic castration-resistant prostate cancer. *Oncologist* **2014**, *19*, 1231–1240. [[CrossRef](#)]
64. Reichenberg, A.; Yirmiya, R.; Schuld, A.; Kraus, T.; Haack, M.; Morag, A.; Pollmächer, T. Cytokine-associated emotional and cognitive disturbances in humans. *Arch. Gen. Psychiatry* **2001**, *58*, 445–452. [[CrossRef](#)]
65. Foster, W.R.; Car, B.D.; Shi, H.; Levesque, P.C.; Obermeier, M.T.; Gan, J.; Arezzo, J.C.; Powlin, S.S.; Dinchuk, J.E.; Balog, A.; et al. Drug safety is a barrier to the discovery and development of new androgen receptor antagonists. *The Prostate* **2011**, *71*, 480–488. [[CrossRef](#)] [[PubMed](#)]
66. Cryan, J.F.; Mombereau, C.; Vassout, A. The tail suspension test as a model for assessing antidepressant activity: Review of pharmacological and genetic studies in mice. *Neurosci. Biobehav. Rev.* **2005**, *29*, 571–625. [[CrossRef](#)]
67. Belovicova, K.; Bogi, E.; Csatlosova, K.; Dubovicky, M. Animal tests for anxiety-like and depression-like behavior in rats. *Interdiscip. Toxicol.* **2017**, *10*, 40–43. [[CrossRef](#)] [[PubMed](#)]
68. Santos, B.G.; Carey, R.J.; Carrera, M.P. The acquisition, extinction and spontaneous recovery of Pavlovian drug conditioning induced by post-trial dopaminergic stimulation/inhibition. *Pharmacol. Biochem. Behav.* **2017**, *156*, 24–29. [[CrossRef](#)] [[PubMed](#)]
69. Santos, F.J.; Oliveira, R.F.; Jin, X.; Costa, R.M. Corticostriatal dynamics encode the refinement of specific behavioral variability during skill learning. *eLife* **2015**, *4*, e09423. [[CrossRef](#)]
70. Li, L.; Kang, Y.X.; Ji, X.M.; Li, Y.K.; Li, S.C.; Zhang, X.J.; Cui, H.X.; Shi, G.M. Finasteride inhibited brain dopaminergic system and open-field behaviors in adolescent male rats. *CNS Neurosci. Ther.* **2018**, *24*, 115–125. [[CrossRef](#)]
71. Navarro-Mabarak, C.; Camacho-Carranza, R.; Espinosa-Aguirre, J.J. Cytochrome P450 in the central nervous system as a therapeutic target in neurodegenerative diseases. *Drug Metab. Rev.* **2018**, *50*, 95–108. [[CrossRef](#)]
72. Belujon, P.; Grace, A.A. Dopamine System Dysregulation in Major Depressive Disorders. *Int. J. Neuropsychopharmacol.* **2017**, *20*, 1036–1046. [[CrossRef](#)]

73. Jardí, F.; Laurent, M.R.; Kim, N.; Khalil, R.; De Bundel, D.; Van Eeckhaut, A.; Van Helleputte, L.; Deboel, L.; Dubois, V.; Schollaert, D.; et al. Testosterone boosts physical activity in male mice via dopaminergic pathways. *Sci. Rep.* **2018**, *8*, 957. [[CrossRef](#)]
74. Fjodorova, M.; Louessard, M.; Li, Z.; De La Fuente, D.C.; Dyke, E.; Brooks, S.P.; Perrier, A.L.; Li, M. CTIP2-Regulated Reduction in PKA-Dependent DARPP32 Phosphorylation in Human Medium Spiny Neurons: Implications for Huntington Disease. *Stem Cell Rep.* **2019**, *13*, 448–457. [[CrossRef](#)]
75. Hussain, M.; Fizazi, K.; Saad, F.; Rathenborg, P.; Shore, N.; Ferreira, U.; Ivashchenko, P.; Demirhan, E.; Modelska, K.; Phung, D.; et al. Enzalutamide in Men with Nonmetastatic, Castration-Resistant Prostate Cancer. *N. Engl. J. Med.* **2018**, *378*, 2465–2474. [[CrossRef](#)] [[PubMed](#)]
76. Moilanen, A.M.; Riikonen, R.; Oksala, R.; Ravanti, L.; Aho, E.; Wohlfahrt, G.; Nykänen, P.S.; Törmäkangas, O.P.; Palvimo, J.J.; Kallio, P.J. Discovery of ODM-201, a new-generation androgen receptor inhibitor targeting resistance mechanisms to androgen signaling-directed prostate cancer therapies. *Sci. Rep.* **2015**, *5*, 12007. [[CrossRef](#)] [[PubMed](#)]
77. Clegg, N.J.; Wongvipat, J.; Joseph, J.D.; Tran, C.; Ouk, S.; Dilhas, A.; Chen, Y.; Grillot, K.; Bischoff, E.D.; Cai, L.; et al. ARN-509: A novel antiandrogen for prostate cancer treatment. *Cancer Res.* **2012**, *72*, 1494–1503. [[CrossRef](#)]
78. Rathkopf, D.; Scher, H. Androgen Receptor Antagonists in Castration-Resistant Prostate Cancer. *Cancer J.* **2013**, *19*, 43–49. [[CrossRef](#)]
79. Sestakova, N.; Puzserova, A.; Kluknavsky, M.; Bernatova, I. Determination of motor activity and anxiety-related behaviour in rodents: Methodological aspects and role of nitric oxide. *Interdiscip. Toxicol.* **2013**, *6*, 126–135. [[CrossRef](#)] [[PubMed](#)]
80. Islam, M.N.; Sakimoto, Y.; Jahan, M.R.; Ishida, M.; Tarif, A.M.M.; Nozaki, K.; Masumoto, K.-h.; Yanai, A.; Mitsushima, D.; Shinoda, K. Androgen Affects the Dynamics of Intrinsic Plasticity of Pyramidal Neurons in the CA1 Hippocampal Subfield in Adolescent Male Rats. *Neuroscience* **2020**, *440*, 15–29. [[CrossRef](#)] [[PubMed](#)]
81. Gibbs, R.B.; Johnson, D.A. Sex-specific effects of gonadectomy and hormone treatment on acquisition of a 12-arm radial maze task by Sprague Dawley rats. *Endocrinology* **2008**, *149*, 3176–3183. [[CrossRef](#)]
82. Kritzer, M.F.; Brewer, A.; Montalant, F.; Davenport, M.; Robinson, J.K. Effects of gonadectomy on performance in operant tasks measuring prefrontal cortical function in adult male rats. *Horm. Behav.* **2007**, *51*, 183–194. [[CrossRef](#)] [[PubMed](#)]
83. Kritzer, M.F.; McLaughlin, P.J.; Smirlis, T.; Robinson, J.K. Gonadectomy Impairs T-Maze Acquisition in Adult Male Rats. *Horm. Behav.* **2001**, *39*, 167–174. [[CrossRef](#)]
84. Moser, M.B.; Moser, E.I.; Forrest, E.; Andersen, P.; Morris, R.G. Spatial learning with a minislab in the dorsal hippocampus. *Proc. Natl. Acad. Sci. USA* **1995**, *92*, 9697–9701. [[CrossRef](#)] [[PubMed](#)]
85. Nilsson, M.; Perfilieva, E.; Johansson, U.; Orwar, O.; Eriksson, P.S. Enriched environment increases neurogenesis in the adult rat dentate gyrus and improves spatial memory. *J. Neurobiol.* **1999**, *39*, 569–578. [[CrossRef](#)]
86. Trouche, S.; Bontempi, B.; Rouillet, P.; Rampon, C. Recruitment of adult-generated neurons into functional hippocampal networks contributes to updating and strengthening of spatial memory. *Proc. Natl. Acad. Sci. USA* **2009**, *106*, 5919–5924. [[CrossRef](#)] [[PubMed](#)]
87. Tramontin, A.D.; Wingfield, J.C.; Brenowitz, E.A. Androgens and estrogens induce seasonal-like growth of song nuclei in the adult songbird brain. *J. Neurobiol.* **2003**, *57*, 130–140. [[CrossRef](#)] [[PubMed](#)]
88. Farinetti, A.; Tomasi, S.; Foglio, B.; Ferraris, A.; Ponti, G.; Gotti, S.; Peretto, P.; Panzica, G.C. Testosterone and estradiol differentially affect cell proliferation in the subventricular zone of young adult gonadectomized male and female rats. *Neuroscience* **2015**, *286*, 162–170. [[CrossRef](#)] [[PubMed](#)]
89. Balthazart, J.; Ball, G.F. Endocrine and social regulation of adult neurogenesis in songbirds. *Front. Neuroendocrinol.* **2016**, *41*, 3–22. [[CrossRef](#)] [[PubMed](#)]
90. Spritzer, M.D.; Galea, L.A. Testosterone and dihydrotestosterone, but not estradiol, enhance survival of new hippocampal neurons in adult male rats. *Dev. Neurobiol.* **2007**, *67*, 1321–1333. [[CrossRef](#)]
91. Pelletier, G. Steroidogenic enzymes in the brain: Morphological aspects. *Prog. Brain Res.* **2010**, *181*, 193–207. [[CrossRef](#)]
92. Kimoto, T.; Tsurugizawa, T.; Ohta, Y.; Makino, J.; Tamura, H.; Hojo, Y.; Takata, N.; Kawato, S. Neurosteroid synthesis by cytochrome p450-containing systems localized in the rat brain hippocampal neurons: N-methyl-D-aspartate and calcium-dependent synthesis. *Endocrinology* **2001**, *142*, 3578–3589. [[CrossRef](#)]
93. McEwen, B.S.; Zigmond, R.E.; Gerlach, J.L. Sites of steroid binding and action in the brain. In *Structure and Physiology*; Elsevier: Amsterdam, The Netherlands, 1972; pp. 205–291.
94. Numakawa, T.; Odaka, H.; Adachi, N. Actions of Brain-Derived Neurotrophic Factor and Glucocorticoid Stress in Neurogenesis. *Int. J. Mol. Sci.* **2017**, *18*, 2312. [[CrossRef](#)]
95. Cirulli, F.; Berry, A.; Chiarotti, F.; Alleva, E. Intrahippocampal administration of BDNF in adult rats affects short-term behavioral plasticity in the Morris water maze and performance in the elevated plus-maze. *Hippocampus* **2004**, *14*, 802–807. [[CrossRef](#)] [[PubMed](#)]
96. Kempadoo, K.A.; Mosharov, E.V.; Choi, S.J.; Sulzer, D.; Kandel, E.R. Dopamine release from the locus coeruleus to the dorsal hippocampus promotes spatial learning and memory. *Proc. Natl. Acad. Sci. USA* **2016**, *113*, 14835–14840. [[CrossRef](#)] [[PubMed](#)]
97. Perreault, M.L.; Shen, M.Y.F.; Fan, T.; George, S.R. Regulation of c-fos expression by the dopamine D1-D2 receptor heteromer. *Neuroscience* **2015**, *285*, 194–203. [[CrossRef](#)] [[PubMed](#)]